NASA TECHNICAL NOTE

NASA TN D-3646

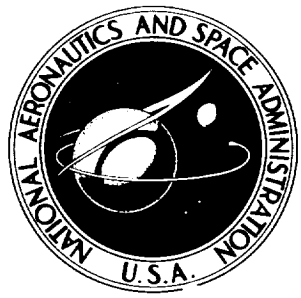

NASA TN D-3646

PROJECT FIRE INSTRUMENTATION FOR RADIATIVE HEATING AND RELATED MEASUREMENTS

by Norman R. Richardson

Langley Research Center

Langley Station, Hampton, Va.

NATIONAL AERONAUTICS AND SPACE ADMINISTRATION • WASHINGTON, D. C. • OCTOBER 1966

NASA TN D-3646

PROJECT FIRE INSTRUMENTATION FOR RADIATIVE HEATING AND RELATED MEASUREMENTS

By Norman R. Richardson

Langley Research Center
Langley Station, Hampton, Va.

NATIONAL AERONAUTICS AND SPACE ADMINISTRATION

For sale by the Clearinghouse for Federal Scientific and Technical Information
Springfield, Virginia 22151 – Price $2.50

CONTENTS

PROJECT FIRE INSTRUMENTATION FOR RADIATIVE HEATING AND RELATED MEASUREMENTS

By Norman R. Richardson
Langley Research Center

SUMMARY

Project Fire was a project of the National Aeronautics and Space Administration which successfully gathered in-flight data on the heating environment of vehicles entering the earth atmosphere at velocities slightly greater than return velocities from a lunar mission. The performance of the standard and specially developed instrumentation was excellent and resulted in a complete recovery of the desired data. A radiometer system and calibration techniques were developed to meet the measurement and accuracy requirements of Project Fire. Within certain limitations discussed in this report, it is considered that radiative heating data were obtained, at the instruments, with an inaccuracy no greater than about ±25 percent of reading.

INTRODUCTION

Project Fire was undertaken by the National Aeronautics and Space Administration to investigate the heating environment of vehicles entering the earth atmosphere at velocities slightly greater than lunar return velocities. The primary objectives of the flight-reentry experiments were to obtain onboard measurements that would define the hot-gas radiance and the total heating on a blunt-nosed body of fairly large scale to provide data anchor points for comparison with results obtained from ground facilities and theoretical prediction methods. Instrumentation was also included for the measurement of body motions, radio signal attenuation, and various ancillary and diagnostic functions.

The two flight tests were successfully conducted on April 14, 1964, and May 22, 1965. Both were launched from Cape Kennedy, Florida, along the Eastern Test Range, with reentries occurring in the vicinity of Ascension Island at velocities in excess of 11.3 km/sec.

The instrumentation of the reentry packages was based on the use of currently available components and techniques whenever possible. The radiometer system for the measurement of the radiative heating was specifically developed to suit the requirements of Project Fire; otherwise the instrumentation was primarily "off the shelf" with some custom packaging or modifications to suit mounting or environmental requirements.

The primary purpose of this paper is to report on the radiometer system and its calibration techniques, both as new developments and in support of the radiation data reports derived from the flight tests. The other instrumentation will be described in less detail with the emphasis on the overall system integration and operation.

FLIGHT PLAN

The reentry package was accelerated to the desired reentry velocity by an Antares solid-propellant rocket motor after being placed in a ballistic trajectory by an Atlas D launch vehicle. Details of the flight plan and vehicle are given in reference 1. A typical pictorial summary of a flight plan and sequence of events is shown in figure 1 for reference. The trajectory and reentry locations were selected to make the optimum use of the existing telemetry, radar, and optical instrumentation on Ascension Island. An instrumented ship located near the impact region provided backup coverage.

Project Fire was planned as a two-flight program with the second flight as a backup. The ensuing description is based on the second-flight instrumentation. The first flight was generally successful although there was not a complete recovery of all the reentry data. A summary of Fire I problems and the resulting corrective measures are given in appendix A.

REENTRY PACKAGE

General Description

The reentry package had a blunt forebody and conical afterbody. Figure 2 is a sectional view of the package. The maximum diameter was about 67 cm and the weight (mass) about 86 kg. Total heating was measured by use of calorimeter techniques, and the radiative heating component was measured with radiometers viewing through quartz windows in the blunt face. Since neither a usable calorimeter material nor a window material could be expected to last through the reentry heating period, a layered forebody construction was used as shown in figure 2. The three beryllium layers were heavily instrumented with thermocouples for use as calorimeters, and each layer provided total heating data until surface melt occurred. Ejectable phenolic-asbestos shields were used to provide heat protection for the second and third calorimeters. These shields were ejected on command, after melt of the preceding beryllium layer, to expose the second calorimeter near the period of peak heating and the third calorimeter as soon thereafter as possible. This arrangement provided three calorimeter data periods in a "clean" environment at time periods that allowed a definition of the reentry-heating envelope. The sequence also provided "clean" windows for the radiometers viewing the gas cap.

Since successful data gathering depended so heavily on the performance of the heat-shield ejection system, it is described in more detail in appendix B.

A grid structure in the forebody provided mountings for the instrumentation and operation system components. The afterbody was connected to the forebody by a bayonet lock and the resulting canister was hermetically sealed to maintain essentially 1 atmosphere internal pressure for the duration of the flight. A closed-loop equipment-cooling system was mounted in the apex of the afterbody. It recirculated the reentry-package air through a heat exchanger using evaporating water as the coolant in flight and freon during ground tests. A photograph of the opened reentry package in the handling fixture is shown in figure 3. Figure 4 is a photograph of the closed package as it was readied for flight.

The Republic Aviation Corporation was the prime contractor for the design, construction, testing, and launch-operation phases of the reentry packages. Two flight articles and a prototype test article were procured.

Data Acquisition and Communications System

Because the reentry packages were not recoverable, all data acquired onboard were telemetered to ground stations by an FM/FM telemetry system using VHF transmitters. Since radio-frequency (rf) blackout could be expected during most of the reentry-heating data period, a data-storage tape recorder was provided to permit delayed transmission of those data after the reentry blackout.

There were a total of 300 sensors or measurement points in the reentry package. A summary list of the primary-experiment measurements is given in table I(a), and a list of supporting measurements is given in table I(b).

Data acquisition.- Figure 5 is a block diagram of the data acquisition system showing the subcarrier assignments. Eleven voltage-controlled oscillators (Inter-Range Instrumentation Group (IRIG) standard frequencies) and a 100-kc crystal-controlled reference oscillator made up the FM multiplex. Time-division multiplexing of four subcarriers was provided by mechanical commutators. The 100-kc reference oscillator was included to permit wow and flutter compensation of data from the onboard tape recorder. A time-code generator was included in the system to provide good real-time correlation of the recorded and replayed reentry data.

Since data would be acquired from each calorimeter in sequence, a considerable increase in data capacity was obtained by connecting only the active calorimeter into the data acquisition system. Three 90×10 commutators, commutator selector switches, an amplifier, and PDM (pulse duration modulation) electronics were built into a single unit. Each calorimeter and the phenolic-asbestos insulation layer behind it had a total of

84 thermocouples which were connected to one of the commutators as indicated. From launch, the output of the first commutator was connected to the amplifier—PDM-keyer combination. The programer commands which initiated the ejection of the two phenolic-asbestos shields also commanded the commutator selector to connect the second and third commutators into the system.

Communications system.- Figure 6 is a block diagram of the communications system. Two 4-W solid-state FM transmitters were used; one transmitted data in real time and operated at 258.5 Mc; the other transmitted data in delayed time and operated at 237.8 Mc. A bidirectional coupler inserted in each antenna lead provided measurements of forward and reverse power. The antennas were single loops operated in the unity mode and mounted in a teflon insulation band set flush into the afterbody. A continuous-loop tape recorder was used to provide the reentry data storage during blackout. The recorder had a loop time of about 45 sec compared with an expected blackout time of about 30 sec. From launch, the recorder was operated continuously in the record-reproduce-erase-record mode. Data from the delay transmitter were the same as those from the real-time transmitter except for the time-delay offset of 45 sec. About 5 sec after the end of blackout, the erase and record heads of the tape recorder were disabled by the reentry timer system. The reentry data were thus retained in storage for continued playback. The flight time available after blackout permitted four playback cycles of the reentry data.

A solid-state modulation switch known as a fail-over switch was used to provide additional redundancy in retrieving the reentry data. A functional schematic of this switch is shown in figure 6. When this switch was actuated about 40 sec after blackout, the real-time transmitter became a delay-time transmitter and both rf links could be used to retrieve the prime reentry data.

Radio-frequency interference filtering.- The reentry-package instrumentation was exposed to a strong rf field since the primary afterbody structure in the antenna region was rf transparent (fiber glass). The requirements and methods for rf shielding and filtering were determined primarily by test with a prototype assembly. The operation of the system showed very severe interference problems, particularly in low-level signal circuits. The system had been wired for a single-point ground; this introduced a large amount of ground wiring which would have been very difficult to shield adequately. Conversion to a local grounding, with the primary grid structure as a ground plane, had a major effect in reducing the interference. Other wiring shielding was improved and bypass filtering was provided with 1000-pF feedthrough capacitors at the input connections of certain components. The entire FM multiplex was encased in a shielding box, and all external connections were made with the feedthrough capacitors. For the PDM commutator system, effective rf filtering was accomplished with bypass capacitors at the amplifier input and the need of filtering every thermocouple lead was avoided. In

a few cases, a small, well-grounded box had to be added over the input connections of an existing component to provide a proper mounting for the capacitors. These modifications, when incorporated into the flight articles, resulted in a very "clean" system with regard to rf interference. This isolation of the reentry-package system from its own rf field probably contributed to the very successful performance of the package during joint operations with the complete space vehicle system.

Tracking System

A C-band transponder beacon was installed in the reentry package as a radar tracking aid. Two antennas and a transfer switch were used to provide the required look-angle coverage. A forward-looking helix antenna was mounted on the reentry-package adapter as shown in figure 2. It was connected to the beacon through a disconnect in the apex of the reentry package. The radiation pattern of this antenna permitted tracking by the Ascension Island radars from horizon acquisition to reentry-package separation. At reentry-package separation, an rf switch transferred the beacon to an antenna array on the package apex which permitted beacon tracking until blackout and continued tracking after blackout.

Reentry-Package Sequence of Events

Figure 7 is a diagram of the sequence-of-events operation for the reentry package. The physical relationship of the three areas and two separation lines indicated can be seen on the flight-plan pictorial in figure 1. An auxiliary battery was mounted in the velocity package to power the instrumentation system from launch through the coast phase and permit the use of a smaller battery in the reentry package. Before spacecraft spin-up, the velocity-package timer system switched the internal battery onto the line and started the separation timers in the reentry-package adapter. This was followed by the first separation indicated, Antares motor burn, and a short coast period before the separation of the reentry package. Tied to the separation of the reentry package were the actuation of the beacon-antenna transfer switch and the enabling of the reentry timing system.

The reentry timing system for the ejection of the heat shields had to be one that would allow for nominal variations in flight time and trajectory. Reentry deceleration was selected as the best and most practical dependent variable for the initiation of the reentry sequence. An acceleration switch, set for -10g, was used to start three solid-state timer modules with time intervals and functions as indicated in figure 7. The acceleration switch was electrically isolated until the reentry-package separation to insure against vibration-induced actuation during the powered phases of flight.

RADIOMETER SYSTEM

The Project Fire radiometer system consisted of three total radiometers and one scanning spectral radiometer. The total radiometers were designed to measure the integrated radiation occurring between 0.2 and about 4.0 μ; the spectral radiometer was designed to scan the radiation occurring between 0.2 and 0.6 μ. One total radiometer, which is referred to as the stagnation total radiometer, was combined with the spectral radiometer in a single case mounted in the forebody at the stagnation location. These radiometers had common fore optics and viewed the same region of the gas cap through quartz windows set into the beryllium and phenolic-asbestos layers. The other two total radiometers were identical units; one was mounted to view forward through windows at an offset location on the forebody and the other was mounted to view through a window in the afterbody wall. The term "offset" will be used in describing both of these total radiometers except where it is necessary to distinguish between them. Figure 8 shows the radiometer and window installation locations in the reentry package.

The radiometer system was developed specifically to meet the measurement and packaging requirements of Project Fire. The packaging density of the reentry package and the time schedule were such that the radiometer envelopes had to be fixed from very preliminary design work and the fabrication of flight hardware started without benefit of a development model. The difficulties of assembly, adjustment, and calibration of the radiometer system were such that it became a primary schedule-pacing item for each flight. The description given herein is based on the system used for Fire II after some modifications to both the instruments and calibration procedures as a result of the Fire I experience; pertinent differences in the Fire I system are summarized in appendix A. Discussion of the radiometer characteristics, calibrations, and accuracies is limited to the instruments themselves and does not include any effects of window attenuation or analysis techniques. Fire I radiometer data and analysis are presented in reference 2.

Definitions and Symbols

The following definitions and symbols are pertinent to the description of the radiometer characteristics and calibration:

Radiometer as used herein denotes an instrument for measuring thermal radiation.

Spectral or monochromatic is used to describe properties or measurements associated with a discrete wavelength or a very narrow wavelength interval.

Total is used when a property or measurement is considered in terms of a broad spectral interval.

Irradiance denotes the quantity of radiant flux in watts incident on a unit area of a real or hypothetical surface in centimeters^2.

Steradiancy defines radiant flux per unit area per unit solid angle. The term is used in defining the emission of a source or the irradiation provided by the source.

Spectral response or spectral flatness is used in describing the wavelength dependence of the characteristics of an element or combinations of elements over a particular wavelength interval.

H	total irradiance, watts per centimeter^2
H_λ	spectral irradiance, watts per centimeter^2-micron
B	total steradiancy, watts per centimeter^2-steradian
B_λ	spectral steradiancy, watts per centimeter^2-steradian-micron
ϵ	emissivity
T	temperature, degrees Kelvin
T_B	brightness temperature, degrees Kelvin
λ	wavelength, microns
τ	apparent transmittance
ω	unit solid angle, steradians

General Characteristics

Ranges.- The usable dynamic ranges, at the instrument, were as follows:

Total radiometers:

0.1 to 100 W/cm^2-sr

Spectral radiometer:

0.1 to 100 W/cm^2-sr-μ

Wavelength range, 0.2 to 0.6 μ

Scan time, 0.1 sec

Resolution, about 40 Å (half-power bandwidth)

Physical.- The dimensions and weights of each component were as follows:

Total radiometer (2) – 42 by 76 by 33.5 mm, 0.34 kg each

Spectral/total radiometer – 102 by 152 by 108 mm, 2.8 kg

Low-voltage power supply – 70 by 112 by 25 mm, 0.3 kg

Electrical.- The electrical characteristics were as follows:

Input power – 28 V dc at 1.0 A

Outputs – 0 to 5 V dc for all channels. All outputs are approximate functions of logarithm of radiation levels.

Optical Design

Total radiometer.- An optical schematic of the offset total radiometer is shown in figure 9 with the central optical rays traced and the forebody windows shown for reference. The principal elements are a thermopile detector and a condensing lens which provided a controlled acceptance field for the detector. This optical arrangement provides a detector output which is a direct function of the steradiancy of any uniform radiating source which fills the conical acceptance field. The lens focal length is such that the detector is imaged at the approximate location shown between the second and third windows in the forebody. The conical acceptance field had an included angle of about 8^{o} which remained well within the diameter of the windows.

The detector was a radiation thermopile (C. M. Reeder Co.) having a 2-mm-square receiver surface made up of four 1-mm-square elements of gold foil with deposited gold black as the absorber. The active and compensating elements were sealed in a small brass housing with the active surface viewing through a 0.5-mm-thick, uv grade quartz window. Sensitivities of the thermopiles were on the order of 15 to 20 $mV/W/cm^2$ and the low mass of the receiver provided a time constant of about 10 msec.

Two subminiature tungsten-filament lamps C were mounted as intensity calibration lamps on the thermopile window. The radiometer signal, when these lamps were energized, was not of sufficient magnitude to provide a good calibration check level; therefore, their principal use was to monitor functional operation during system testing.

The folding mirror was used to reduce the length of the unit for packaging reasons. The schematic shown in figure 9 is for the offset location on the forebody; the afterbody installation was identical except for the window arrangement. Within the envelope indicated were included the primary electronics and the rf filtering.

Spectral/total radiometer.- A total radiometer and the spectral radiometer were combined into one package for installation at the stagnation location. The total radiometer was essentially the same as the individual total radiometers described previously. The spectral radiometer was a scanning double monochromator with a rocking grating

used as the primary dispersing element and a prism used primarily to divert the overlapping second order. The case of the combined instrument also housed power distribution and control functions for the other two total radiometers.

Figure 10 is a photograph of the spectral/total radiometer removed from its case. The instrument was constructed in a three-deck configuration. The top deck contained the photomultiplier detector, the high-voltage power supply, and the electronic modules; the center deck contained the optical elements and the total-radiation thermopile; the lower deck contained the grating and prism drive cams, the motor with associated gearing, a mechanical commutator, and the electronic modules. Figure 11 shows the first deck removed to expose the optical deck, and figure 12 is an optical schematic with the principal elements identified and the forebody windows shown for reference.

The quartz lens pair L_1 served as the fore optics for both the total and spectral channels. The quartz beam splitter B was aluminized for about 50-percent reflectance and divided the incoming radiation between the total-radiation thermopile T and the monochromator entrance slit S_1. The thermopile and entrance slit were at the same distance from the lens pair and both were imaged at the approximate location indicated between the second and third heat-shield windows. The field for each radiometer channel was about 10° and was always within the diameter of the heat-shield windows.

In the optical schematic (fig. 12), the central ray is traced from the entrance slit to the photomultiplier detector with the grating and prism in the 0.6-micron positions. The four mirrors, M_1 to M_4, are identical off-axis paraboloids. Mirror M_1 has its focus at the entrance slit S_1; M_2 and M_3 have their foci at the intermediate slit S_2; and M_4 has its focus at the exit slit S_3. Thus M_1 and M_3 act as collimators for the rays coming through S_1 and S_2, respectively, while M_2 and M_4 focus these rays at S_2 and S_3, respectively.

The grating and prism holders were mounted in bearings and oscillated through the required angular ranges, by spring-loaded crank arms riding on two peripheral cams mounted on a 5-rps drive shaft. The angular relationship of cam rotation to spectral scan was as follows:

0° to 162°	0.6 to 0.2 μ
162° to 180°	dwell at 0.2 μ
180° to 342°	0.2 to 0.6 μ
342° to 360° (0°)	dwell at 0.6 μ

The grating was a 600-line/mm replica blazed for 0.4-μ first order and acted as the primary dispersing element. Its drive cam was cut with an essentially linear rate of rise so that the spectrum was scanned linearly with cam rotation (time) across the intermediate slit S_2. The prism was driven through an angular range which provided a

constant total deviation for the first-order wavelength incident from the intermediate slit, while diverting the overlapping second order away from the exit slit. The entrance slit, intermediate slit, and grating geometry were designed to provide an optical resolution (half-power bandwidth) of about 20 Å; measurements made from radiometer scans of a mercury-lamp source indicated that the effective half-power bandwidth was more nearly 40° Å. A large part of this broadening appeared to be caused by electronic recovery time after a pulse input. The exit slit S_3 more appropriately could be called a baffle since it was optically very wide to relieve the optical tracking requirements and served primarily to block the dispersed second-order and other stray light. Also, since this slit was very wide, the radiometer maintained a relatively constant bandwidth unaffected by the non-linear dispersion of the prism. Imperfect tracking in the Fire II radiometer caused the image to traverse the exit slit and resulted in a cut-off of the ultraviolet wavelengths below about 0.26 μ. The difficulty of making adjustments in such a compact instrument and the shortage of time precluded any attempts to recover this part of the scan. The exact wavelength at which occlusion began was difficult to determine; for flight use, the instrument was considered usable only down to 0.3 μ to avoid the uncertain end of useful wavelength range.

Two calibration lamps were mounted as shown in figure 12. The intensity calibration lamp C_2 was a small neon lamp located so that some of its light would be received directly by the photomultiplier. It was energized during part of the scan dwell time at 0.2 μ to provide a calibration reference level for the photomultiplier and electronics. The spectral calibration lamp C_1 was a continuously illuminated mercury-vapor lamp imaged at the entrance slit off the back side of the beam splitter, the intent being to have a known spectrum at low levels displayed in the output as a continuous scan-time—wavelength calibration check. There was difficulty both in obtaining a fully suitable lamp and in achieving the desired signal level for the lamp spectrum. The scan-wavelength calibration appeared to be adequately repeatable so that the lamp was not needed as a primary calibration source; however, it was considered of value to verify functional operation of the scanning mechanism during system testing.

Radiometer Electronics

The radiometer electronics were completely redesigned for the Fire II system. Originally the radiometer was designed with dc amplification of the low-level detector outputs; the redesigned system used ac amplifiers which provided greater stability of operation. The radiometer system was designed to operate with a single 28-V dc input from the instrumentation power bus. A low-voltage power supply, with a 17-kc inverter, was used as a dc-dc converter to provide the bias voltages for the various amplifiers. The power-supply inverter also had a 70-V output at 17 kc as the driver for the

high-voltage power supply required for the photomultiplier. Regulation was provided at the inverter, and critical voltages were also monitored in flight. A power-distribution diagram for the system is shown in figure 13. A block diagram of the signal and control circuits for the spectral radiometer and one of the three total radiometers is shown in figure 14.

Total radiometer.- A specially designed magnetic modulator (magnetic amplifier) operating in a linear portion of the hysteresis loop was used to convert the thermopile output to an ac signal for amplification. The output of the radiation thermopile was about 30 mV at the full-scale level. The thermopile voltage, after preamplification, was fed to the signal (control) winding of the magnetic modulator. A 27-kc oscillator provided the modulation drive for each magnetic modulator. The amplitude-modulated output of the magnetic modulator was coupled to an ac amplifier followed by a diode detector and output filter network. The low-pass characteristics of the filter provided an output signal that was essentially noise free. The forward characteristics of two silicon reference diodes in series at the detector output provided a logarithmic feedback signal to the feedback winding of the magnetic modulator. The system operated as a linear amplifier until the reference diodes began to conduct at about 1.5 V; from 1.5 V to the full scale of about 4 V the output was approximately a function of the logarithm of the thermopile voltage.

Spectral radiometer.- The detector for the spectral radiometer was a miniature version of a ruggedized 14-dynode photomultiplier (Ascop 541A-05-14) having a cesium-antimony photocathode and a sapphire window. The tube was modified from its normal configuration by the addition of an external connection to the seventh dynode, which was not connected to the dynode divider network. This dynode was modulated by the 27-kc oscillator through appropriate circuitry; the output from the photomultiplier was then an amplitude-modulated 27-kc signal. This signal was coupled to an ac amplifier followed by a diode detector and filter network. The low-pass output filter was designed to be flat up to about 3 kc to provide adequate frequency response. Power supply and modulation frequencies were selected with consideration for the output-filter characteristics; however, harmonics generated in the electronics resulted in some residual noise in the output. From a relatively quiet base line, the noise envelope increased to about 0.3 V peak-to-peak at midscale. Logarithmic compression of the output was provided by the forward characteristics of a reference diode at the detector circuit. The output was a linear function of photomultiplier signal until the reference diode began to conduct at about 0.75 V and was approximately a logarithmic function from 0.75 V to the full-scale output of about 4.5 V.

Drive and switching.- A permanent magnet motor, through gearing, drove the prism and grating cam shaft at a nominal speed of 5 rps. A multiwafer, two-speed, commutator was coupled to this shaft to provide calibration and zero functions for each radiometer

channel. For the spectral radiometer the commutator operated at 5 rps. Commutator switch 1 was opened for approximately the first half of the 18° dwell at each end of the spectral scan to provide a telemetry zero reference. During the remainder of the dwell at 0.6 μ, switch 2 was closed to provide a telemetry 5-V full-scale calibration signal. Switch 3 was closed during the dwell at 0.2 μ to energize the intensity calibration lamp. Other commutator wafers, geared to 0.5 rps, provided the same calibration functions for each total radiometer.

Spectral-Response Characteristics

The total radiometers were used to measure the integrated radiation over a certain wavelength range and therefore should have a reasonably uniform response to any radiation within this range; consequently, the spectral characteristics of each contributing element must be known and evaluated for their effect on the accuracy of both the radiometer calibration and the flight data. Transmission cut-off by the quartz windows at about 0.2 μ set the lower limit of concern for total-radiometer response; the radiation measured in flight was expected to occur primarily below 2 μ which was the upper limit of primary concern. The contributing elements in the total radiometer were a lens, a mirror, and the detector. Each element was chosen from available materials which generically should provide the desired spectral characteristics. Specific tests have been conducted, where possible, to determine the characteristics of the actual elements used. The types of tests conducted are described here and the spectral response summation is discussed in a succeeding section entitled "Radiometer Measurement Accuracy."

Lenses.- The lenses used in the radiometers were made from a uv grade of fused quartz (Corning No. 7940). Vendor's data on the apparent transmittance for this material were used in deriving the spectral characteristics of the total radiometers.

Mirrors.- The mirror for the stagnation total radiometer (fig. 12) was a beam splitter having a semitransparent film of aluminum deposited on a quartz substrate for about 50-percent reflectance. The mirror for each offset total radiometer was aluminum evaporated on a quartz substrate and overcoated with magnesium fluoride. Relative measurements of spectral reflectance were made for these mirrors during the period of radiometer assembly. The beam splitter for the flight article and the spare radiometer were both tested and found to have the same characteristics. Measurements were made on one of the offset-radiometer mirrors as a "witness sample"; it was coated simultaneously with the flight article mirrors and installed in the spare offset radiometer.

Absolute reflectance measurements were made at the Langley Research Center on the mirrors from the spare instruments. These measurements were made in a recording spectrophotometer with an integrating sphere reflectance attachment. The instrument was of the dual-beam configuration and fresh magnesium oxide was used as the reference.

These measurements were in general agreement with the earlier relative measurements and were used in deriving spectral response characteristics for the total radiometers.

Detectors.- The total-radiometer detectors, as previously described, were thermopiles having gold-black-surfaced receivers. A precise spectral-response calibration of a thermopile is very difficult to obtain because of the lack of readily available reference standards of known response. Tests such as those covered in the literature have indicated that the gold-black detector generically exhibits a reasonably flat spectral response (better than 90 percent) in the wavelength region of about 0.2 to 2.5 μ, which is the range of concern in this application. In an effort to verify nominal characteristics for the detectors, relative response tests were conducted on each one used. These measurements were made with a Perkin-Elmer model 99 monochromator modified to permit the use of a high-output mercury-lamp source. The reference detector was a Perkin-Elmer instrument-type thermocouple with a gold-black detector surface and a potassium bromide window. A mirror was arranged so that the monochromator beam could be directed to either the reference detector or the test item, and output records for each were made at 17 different wavelengths between 0.26 and 2.9 μ. The ratios of the test-item output to reference-detector output for each wavelength were averaged to obtain an average sensitivity ratio; the deviation of the individual wavelength ratios from this average was then converted to a percentage deviation from the average. Data derived by these means for the three detectors used in the radiometer system are shown in figure 15 and indicate no particular trend of spectral-response variation with respect to the reference detector. The maximum variation for any data point was about 9 percent and the majority of the data points showed relative response deviations of no more than 5 percent. Although these tests were relative, they did indicate a nominal and consistent spectral response for the detectors.

An additional relative response test was subsequently conducted at the Langley Research Center on a spare detector. For these tests, a 1000-W tungsten-coil projection lamp followed by a double-prism monochromator was used as the source; a laboratory thermopile having a lamp-black receiver surface was used as the reference; and a millimicrovoltmeter was used to measure the thermopile outputs. The source was "calibrated" at a series of 18 different wavelengths from 0.395 to 1.87 μ by use of the lamp-black reference thermopile. The reference thermopile was then replaced by the gold-black thermopile and the output measured at the same 18 wavelengths. The ratios of the outputs at each wavelength were averaged and treated as described in the preceding paragraph. Again there was no trend of response variation and the majority of the individual variations from the average were less than 5 percent.

RADIOMETER SYSTEM CALIBRATION

A calibration of the total and spectral radiometers is required to generate curves relating absolute source steradiancy to radiometer output voltage. The basic requirements for the calibration apparatus were as follows:

(1) A stable source of uniform steradiancy which would completely fill the acceptance field of the radiometer at a level high enough to provide calibration increments as near full scale as possible

(2) Means of accurately measuring the source on an absolute basis and of attenuating the source to provide a series of calibration levels

(3) For the total radiometers, a source having a known spectral distribution which fell within the usable spectral-response range of the radiometer

(4) For the spectral radiometer, monochromatic sources of known wavelengths and steradiancies over the scanning range of the radiometer to provide a calibration of its relative spectral sensitivity

The evolution and evaluation of the calibration apparatus and procedures to meet these requirements was a very difficult technical task. There are limitations both in obtaining adequate sources of radiation and in means of making accurate absolute measurements of the sources, particularly for the high levels required by Project Fire. Continuing evaluation of the calibration apparatus and procedures, in the period between the first and second flights, uncovered many potential sources of error and suggested modifications and additions to improve the probable accuracy of the calibrations. The following description of the calibration procedures attempts to show the extent to which every element in the calibration was, and had to be, considered and evaluated. Differences in the calibration procedure for Fire I from that for Fire II and some of the errors subsequently discovered are described in appendix A.

Two sets of calibration apparatus were developed by the contractor. One used a carbon block in a carbon-tube furnace as the radiation source and is referred to as the furnace or continuum calibration apparatus. The other used a mercury-xenon arc lamp as the source and is referred to as the arc or monochromatic calibration apparatus. In each apparatus, an optical system was used to bring the source emission into a controlled field suitable for an absolute steradiancy measurement and for a radiometer calibration source. A series of filters of known transmittances were used to attenuate the calibration source to obtain a series of calibration levels.

Total-Radiometer Calibration

A photograph of the furnace apparatus used for the calibration of the total radiometers (and part of the calibration of the spectral radiometer) is shown in figure 16. A diagram of the basic elements and optical path is shown in figure 17, which is to scale except for a considerable foreshortening of the furnace tube length and pyrometer location. The radiation source was a heated carbon block in an inert-atmosphere carbon-tube furnace operated at temperatures around 2800° K. Radiation from the block was converged by the lens L_1 to an image at the field stop S_1 where the diameter was adjusted to block the direct rays from the furnace wall out of the following optical path. This image in turn was relayed by the lens L_2 to the plane P. The fixed exit pupil stop S_2 limited the rays reaching this image to a cone with the apex angle θ (referred to hereinafter as cone θ). A measurement was made of the absolute steradiancy of the energy within this cone θ which served as the radiometer calibration source. The angle θ was about 12° and the diameter of the image was about 12 mm to insure complete filling of the radiometer acceptance field with some margin.

Steradiancy determination.- The geometry of the cone θ and the irradiance at the image of the carbon block were used to determine the absolute steradiancy of the energy in the cone θ as a radiometer calibration value. With the furnace at a stabilized temperature, the reference thermopile T was positioned with its receiver surface in the image and the irradiance in W/cm^2 was determined from the thermopile output. (See appendix C for a description of this thermopile and its absolute calibration.) The total steradiancy at the image was then computed in W/cm^2-sr from the relation

$$B = \frac{H}{\omega}$$

For the relatively small angle involved, ω was computed with sufficient accuracy from the approximate relationship

$$\omega = \pi \tan^2 \frac{\theta}{2}$$

Steradiancy uniformity.- The steradiancy in cone θ should be uniform since the calibration steradiancy determination is an average for a field larger than that accepted by the radiometer. Reference thermopile measurements were made with the normal exit pupil stop in place and with it replaced by one larger diameter and two smaller diameter stops. The steradiancy was determined for each condition and was found to be uniform within about 1 percent over the range covering the radiometer acceptance field and the fixed angle used for calibration steradiancy measurements.

Filters.- Neutral-density filters were used singly and in pairs at the locations shown in figure 17 as attenuators to provide a series of calibration steradiancy levels. The filters were made of evaporated inconel on a quartz substrate with decimal transmittances ranging from 0.8 to 0.01 in nine steps. This set of filters was used on a total transmittance basis for the total radiometers and on a monochromatic transmittance basis for the spectral-radiometer calibrations. The filters were always tilted as indicated in figure 17 to divert reflected rays out of the optical path.

Two different transmittance calibrations were made for each filter. The transmittances were first measured at several wavelengths from about 0.25 to 2.3 μ in a recording spectrophotometer and are listed in table II. These data provided transmittance values for the discrete wavelengths used in the spectral-radiometer calibrations and provided a measure of the degree of flatness, or neutral density, over the wavelength range of concern. Total transmittance of each filter was measured with the furnace continuum used as the source. The transmittances were established from an average of many reference thermopile readings taken as the filters were inserted singly and in pairs at their normal location in the furnace calibration apparatus. The average values were used during the total-radiometer calibrations and are also listed in table II.

Calibration procedure.- Before the start of an actual radiometer calibration, the furnace was brought up to temperature and allowed to stabilize for a few hours. The optical pyrometer indicated in figure 17 was positioned to permit measurement of the image brightness temperature, periodically during a test, to monitor the stability of the furnace temperature. The reference thermopile was then inserted at the image plane and from its measurement the source steradiancy was determined as described. The maximum irradiance available at the image was enough at least to deteriorate, if not burn out, the thermopile; consequently, it was only used when filters of a net 20-percent or less transmittance were inserted in the optical path. Normally, measurements were made with most of the filter combinations to be used in the radiometer calibration as a recheck of the filter transmittances. For each combination, the unattenuated source steradiancy was then computed from the relation

$$B = \frac{H}{\omega\tau}$$

where τ is decimal transmittance of filter or product of filters.

After the calibration source was thus standardized, the reference thermopile was removed and the radiometer was positioned so that its optical axis was alined with the calibration apparatus axis and its detector image was about coincident with the carbon-block image. A set of 20 calibration data points, ranging from 100 percent to about 0.08 percent of maximum source steradiancy, were taken using the filters singly and in

combination. At each calibration level, the radiometer output voltage was monitored on an oscilloscope and recorded on an oscillograph for subsequent reduction and construction of the radiometer calibration curve. A typical calibration curve for a Fire II total radiometer is shown in figure 18.

Field of view.- The radiometer field of view was checked by the use of an adjustable diaphragm stop mounted in place of the fixed exit pupil stop. At some convenient steradiancy level, the stop diameter was gradually reduced until a slight reduction in the radiometer output voltage could be detected. From this measurement, the radiometer acceptance field was determined and found to agree well with that indicated by a ray tracing of the radiometer optics. The test also confirmed that the cone of rays provided by the fixed stop adequately overfilled the radiometer acceptance field.

Electrical calibration.- In the final stages of assembly, each total radiometer was electrically calibrated by inserting a controllable voltage source across the proper impedance in place of the thermopile. This calibration provided a curve of the electrical input-output characteristics of the electronics including the shaping of the logarithmic compression circuit; assuming linear response of the thermopile, this should provide the same curve shape as for the optical calibration. Initially, this electrical calibration was made to allow a valid extrapolation of the optical calibration since the maximum steradiancy expected of the calibration apparatus was only about 50 percent of the full-scale range of the radiometers. The information was also of value in confirming the incremental accuracy of the optical calibration.

Calibration steradiancy cross-check.- In an optical train such as that used in the calibration apparatus, the steradiancy at the calibration image field is the same as it is at the carbon block except for the losses at the intervening optical elements. Thus, if the temperature and emissivity of the carbon block and the optical characteristics of the lens materials are known, it is possible to compute the steradiancy at the image as a check of the thermopile-geometry determination. Before making this computation the following assumptions were made:

(1) The radiation emitted by the carbon block had a gray-body distribution.

(2) The effective emissivity of the carbon block was taken as 0.9. The temperature of the furnace wall was the same as that of the carbon block for at least 1 or 2 block diameters; thus a shallow cavity was created which had an effective emissivity greater than the individual block or wall emissivities as discussed in reference 3. The estimate of an emissivity of 0.9 was based on the available information on the high-temperature emissivity of carbon and the cavity effect.

The optical pyrometer reading taken in the course of the calibration was first corrected to obtain the actual block temperature by use of the relation

$$\frac{1}{T} - \frac{1}{T_B} = \frac{\lambda}{C_2} \ln \epsilon_\lambda$$

where λ is the wavelength at which brightness temperature is measured, here 0.65 μ; C_2 is the second radiation constant, 1.439 cm ^{o}K; and ϵ_λ is the emissivity of the source (or transmittance of optical elements) at wavelength λ. The apparent transmittance for the furnace window and each lens was taken as 0.93. With the assumed emissivity of 0.9, the factor ϵ_λ became $0.93^3 \times 0.9 = 0.73$. For a typical calibration test, the measured brightness temperature of 2840^{o} K was corrected to 2961^{o} K as the actual block temperature.

The temperature of the block having been determined, the spectral steradiancy of emission was determined by use of the Planck equation. Included in figure 19 are curves of the apparent spectral transmittance of the optical elements and the spectral steradiancy of the source for a temperature of 2961^{o} K and assumed gray-body distribution and 0.9 emissivity. The lowest curve in figure 19 is the spectral steradiancy at the calibration image and is derived from the product of the source steradiancy and transmittance curves. An integration of the area under the derived curve indicates a calibration image steradiancy of about 86.5 W/cm^2-sr. For the same calibration run, the steradiancy determined by the thermopile and geometry measurement was 81.3 W/cm^2-sr. On another run, at a calculated block temperature of 2633^{o} K, the integration gave a calibration steradiancy of 51.7 W/cm^2-sr while the thermopile measurement gave a steradiancy of 55.1 W/cm^2-sr. The total-radiometer calibration values were based on the thermopile-geometry measurements; the ±6-percent agreement with the integration of the gray-body distributions was considered to be a good cross-check of the measuring techniques.

Field and installation checks.- A spare total radiometer was calibrated in the same manner as were the flight articles for use in the field as a means of standardizing a radiometer test source. This test radiometer was simplified by the elimination of the electronics and a direct mV readout of the thermopile. The calibration of this radiometer indicated an excellent combined linearity of the thermopile output and the incremental accuracy of the calibration increments provided by the filters. At the launch site, a 650-W flood lamp was calibrated with this test radiometer and found to have a reasonably uniform steradiancy of about 12 W/cm^2-sr. The lamp was then used alone and with two of the filters described previously to provide calibration checks for the radiometers immediately before installation in the reentry package. After the radiometers were installed, the lamp was again used to check the radiometer performance and verify the pointing alinement through the windows and the combined window transmittance. The agreement with the laboratory calibrations was generally within about 10 percent and thereby provided a good confirmation of stable operation of the radiometers and of proper installation.

Spectral-Radiometer Calibration

Several curves are required to define the calibration of the spectral radiometer compared with the single curve required for a total radiometer. The response of the radiometer was known to vary considerably with wavelength, largely as a function of the spectral sensitivity of the photomultiplier. This variation results in a family of absolute-sensitivity curves which were reduced to a single curve of the absolute sensitivity at a wavelength of maximum spectral sensitivity plus a curve of the relative spectral sensitivity with wavelength. In addition, curves of wavelength as a function of scan interval were developed.

Calibration with monochromatic source.- The apparatus shown in figure 20 was developed for calibration of the spectral radiometer at several wavelengths within the radiometer scan range. The radiation source was a 1000-W mercury-xenon arc lamp followed by a grating monochromator having a 20-Å bandwidth to match the nominal optical bandwidth of the spectral radiometer. The remaining optical system and measuring techniques were similar to those used for the continuum calibration apparatus if the monochromator exit slit is considered to be positioned at the field-stop location of figure 17. The reference thermopile used for the image irradiance measurements in this apparatus had a gold-black receiver surface which was 0.2 mm wide by 2.0 mm long to suit the geometry of the narrow slit image. The geometry of the cone θ and the measured irradiance at the image defined the total steradiancy of the calibration field. The spectral steradiancy in $W/cm^2\text{-}sr\text{-}\mu$ was derived from the relation

$$B_\lambda = \frac{H}{\omega \Delta\lambda}$$

where $\Delta\lambda$ is the wavelength interval, in this case 0.002 μ. This derivation, it should be noted, does not necessarily reflect the true spectral steradiancy of the calibration source which may consist primarily of a mercury line; instead, it treated the source as though it was a radiation band of the equivalent total power distributed uniformly across the 0.002-μ interval. The radiometer similarly indicates the equivalent power rather than the true spectral steradiancy when it scans line or narrow-band radiation occurring in an interval less than the optical bandwidth of the radiometer. Consequently, to provide calibration steradiancies compatible with the radiometer measuring characteristics, the spectral steradiancy of the calibration source must be defined in terms of a wavelength interval which is the same as the optical bandwidth of the radiometer.

Calibrations were made at the six primary mercury lines between 3125 and 5790 Å to provide data on the variations of spectral response in the wavelength scan range of the radiometer. The previously described filters were used singly and in pairs to provide a series of calibration increments. The radiometer output was displayed on an oscilloscope

from which voltage amplitude readings were taken for each steradiancy level as the radiometer scanned the calibration wavelength. A calibration cross-check of the spectral radiometer was then made with the furnace continuum used as the source. The check points disagreed with the monochromatic source calibrations by nearly an order of magnitude. Since the evaluation of absolute accuracy and uniformity had been much more extensive for the continuum source than for the monochromatic source, it was decided to base the final absolute steradiancy calibration of the spectral radiometer on data taken with the continuum source.

Subsequent tests of the monochromatic calibration apparatus showed significant sources of error. The optical geometry of the apparatus had been changed from that previously used with the result that the radiometer acceptance field was considerably underfilled by the available calibration field (cone θ). This fact was not readily apparent from the radiometer field-of-view measurements with the adjustable exit pupil stop; the indicated radiometer field of view was later found to be a function of the limiting system aperture controlled by the monochromator optics at the source. A survey of the monochromator slit image showed that the gradient across the mercury-arc source resulted in a nearly triangular distribution of irradiance along the length of the image; as a result, the irradiance indicated by the very small reference thermopile at the center of the image was about twice as great as the average across the length required to cover the coincident image of the radiometer entrance slit. These two factors, to the extent they were evaluated, appeared large enough to account for a large part of the differences between the calibrations using the monochromatic and continuum sources.

Some redesign and rearrangement of this apparatus would have improved it considerably; however, it appeared that it would always be difficult with the arc source to achieve either a uniform steradiancy over a large enough field or an adequate means of measuring the average steradiancy over the required field. Further analysis of this monochromatic calibration technique indicates several additional factors which affect accuracy and must be considered. These would include: the spectral distribution of the calibration source within the band-pass of the calibration monochromator; the interplay between the slit functions and bandwidths of the monochromator and the radiometer; the assurance that the radiometer instantaneously accepts all the measured total steradiancy of the source; and the proper assignment of the wavelength interval in the conversion of the measured total steradiancy to an effective spectral steradiancy. The difficulty of making an exact analysis of these several factors indicates a strong requirement for a method of cross-checking this calibration technique and a preference for the use of a continuum source for the absolute calibration of the spectral radiometer.

Calibration with continuum source.- The absolute steradiancy calibration of the spectral radiometer was based on measurements made with the furnace continuum used

as the source. For these calibrations, the furnace was operated at its maximum stable temperature to provide as much energy as possible in the spectral range of the radiometer. A simultaneous calibration run was then made on the spectral radiometer and the combined total radiometer with the output of each channel recorded on an oscillograph. A reproduction of typical oscillograph records is shown in figure 21, figure 21(a) being the continuum calibration record.

The derivation of the spectral steradiancy distribution of the calibration source was described previously. Calibration values of spectral steradiancy B_λ were taken at selected wavelengths (the same as used for the monochromatic calibration) from the lowest curve in figure 19 and matched with the appropriate locations in the continuum scan record for reduction. In the scanning range of the spectral radiometer, the maximum spectral steradiancy available from the source was considerably less than the full-scale range of the radiometer; also, below about 0.35 μ there was not enough energy to allow a definition of the relative spectral response of the radiometer. The relative-spectral-response curves derived from the continuum and mercury-arc calibrations in the wavelength range from 0.6 to 0.35 μ were nearly the same; therefore, it was considered valid to use the mercury-arc calibration data as an indication of the relative spectral response between 0.35 and 0.3 μ. Additional confirming data in this wavelength range are available from the initial continuum-calibration cross-check; at that time, the radiometer sensitivity was much greater than it was during the final calibration. The spectral-response curve for the Fire II spectral radiometer is shown in figure 22. The curve in the region from 0.35 to 0.3 μ is dashed since the data for this region are not considered to be as definitive as those for the other wavelengths.

Absolute calibration extension.- A relative calibration of the input-output transfer function of the electronics was made for extension of the absolute calibration to full scale. The radiometer was arranged on the monochromatic calibration apparatus so that the photomultiplier could be irradiated directly rather than through the radiometer optics. The source was then adjusted so that the voltage output of the radiometer electronics was at full scale. From this 100-percent level, the source was attenuated by filters and the radiometer output noted at each level until the voltages had adequately overlapped the range of the absolute calibration. The resulting relative-sensitivity curve was then matched to the overlapping region of the absolute curve to provide a full-scale calibration curve. This curve for the Fire II spectral radiometer is shown in figure 23 for the wavelength of 0.435 μ, which is in the region of maximum spectral response. For any other wavelength, a spectral steradiancy derived from this curve must be divided by the appropriate relative response factor found in figure 22.

Wavelength-scan interval calibration.- The spectral radiometer was irradiated by a mercury lamp and the output recorded on an oscillograph. A sample of such a record

is reproduced in figure 21(b) with the primary mercury lines identified. The leading edges of the 5-V calibration pulse and the intensity calibration pulse were used as the fiducial points in the wave train for the beginning and end of scan. The locations of the known mercury lines were determined in percent of scan interval and used to obtain the wavelength calibration shown in figure 24.

Radiometer Measurement Accuracy

Total radiometers.- The accuracy of the total-radiometer measurements obtained in flight (at the instruments) is a function of the calibration accuracy, instrument stability, and telemetry system accuracy. It is also a function of the spectral flatness of the radiometer. For the calibration of the total radiometers, the cross-checks of the calibration steradiancy indicate that the total steradiancy was being determined with an inaccuracy of less than ±10 percent. The small variations of spectral transmittance of the filters used during the calibration compromise this accuracy to some extent because of the resulting distortion of the spectral distribution of the source. Field checks and in-flight performance indicated no degradation in the radiometer calibration stability. The in-flight accuracy of the radiometer output signal is estimated to be within ±15 percent of reading. The error introduced by telemetry transmission is considered to be no more than ±2 percent (±0.1 V) since each radiometer output carried telemetry calibration signals. A ±0.1 V telemetry error applied to the nearly logarithmic radiometer calibration results in radiation measurement errors of as much as ±15 percent of reading. A root-mean-square summation of the calibration and telemetry errors indicates a probable error of no more than about ±21 percent of reading for the flight measurements exclusive of spectral-response considerations.

Relative-spectral-response curves for the stagnation and offset total radiometers are shown in figures 25 and 26, respectively. These curves are based on the mirror reflectance and lens transmittance which are also shown in each figure; the variations found in detector response were too random to be used in deriving the response curves and are considered to add an uncertainty band of about ±5 percent to the curves. In the region from 0.2 to 2.0 μ, the stagnation total radiometer has a large variation in spectral response due to spectral-reflectance variations of the beam splitter. Several repeat tests were made to confirm this reflectance variation and some supporting evidence can be found in reference 4. Since the spectral-response variations extend across the spectral distribution of the calibration source shown in figure 19, the absolute calibration of the radiometer then is only correct for that distribution or for some monochromatic equivalent. The absolute level of the response curve, which was derived from the product of the reflectance and transmittance curves, has been normalized to satisfy the condition

$$\int B_\lambda F_\lambda \, d\lambda \approx \int B_\lambda \, d\lambda$$

where B_λ is the spectral steradiancy of the calibration field and F_λ is the spectral-response factor for the radiometer and has a mean value of 1.0. The wavelengths at which the response curve has a value of 1.0 are then the monochromatic equivalents of the source continuum and are the wavelengths at which the absolute calibration of the particular radiometer is correct. The ability to make data corrections for the spectral-response variations, of course, depends on a knowledge of the spectral distribution of the radiation source being measured and will influence the final measurement accuracy; the determination of the necessary corrections is a part of the flight-data analysis and is not presented in this report.

Spectral radiometer.- The absolute calibration of the spectral radiometer was probably less precise than that of the total radiometers because it involved more extrapolation and because of the random-noise content in the electrical output. In the range where the flight data occurred, the probable error is estimated to be no greater than ±20 percent of reading. The probable telemetry-system error contribution is about ±15 percent as for the total radiometers. A root-mean-square summation of the two error sources indicates a probable error of no more than about ±25 percent of reading. This statement of accuracy, it should be noted, only applies to the measurement of power rather than correct amplitude for wavelength bands narrower than the bandwidth of the radiometer; also, there may be some degradation of accuracy below 0.35 μ as noted previously in the definition of spectral response in the region from 0.35 to 0.3 μ.

TOTAL HEATING INSTRUMENTATION

Forebody Calorimeters

The three forebody layers of beryllium were instrumented with thermocouples in depth and used as thick calorimeters for the measurement of the total (convective plus absorbed radiative) heat transfer during three periods of the reentry. The pertinent properties of the beryllium and analysis of the Fire I data are presented in reference 5; the following description is concerned with the details of the thermocouple installations, wiring, and check-out.

Thermocouple plugs.- The thermocouple installations were designed to provide the minimum feasible disturbance of the local heat flow with a technique that provided accurate depth control of the thermocouple junction locations. Four chromel-alumel thermocouples were mounted at controlled depths in beryllium plugs which were inserted into the beryllium calorimeters. Twelve plugs were installed in each calorimeter in a pattern of four radii on each of three equally spaced radials; this arrangement provided a considerable degree of redundancy since there were three plug locations at each radius.

The pertinent details of a thermocouple plug are shown in figure 27. The thermocouple mounting core was machined on the end of a rod which served as a mandrel for handling and installation. The core and the sleeve were made from the same billet used for the beryllium dishes to insure identical material properties. Three thermocouple junctions were installed in grooves, as indicated, at nominal distances of 0.3, 1.8, and 3.3 mm from the front face; the fourth junction was welded on the back face of the core. A weld bead was first formed on the small thermocouple wires and then resistance welded into the forward end of each groove. The distance from the mandrel shoulder to the center of each junction bead was measured under a microscope and recorded for every junction. The core was then pressed into the sleeve, with a shrink fit, until the mandrel shoulder was in contact with the finished face of the sleeve. Each thermocouple bead was made to protrude very slightly above the surface of the core so that the pressure of the sleeve would provide mechanical reinforcement of the marginal strength beryllium weld. Small ribbon-strip terminals of chromel and alumel were ceramic cemented into shallow grooves on the rear face of the sleeve. The 0.025-mm thermocouple wires were welded to the inboard ends of these strips and the area was potted with ceramic cement to complete the plug assembly. Figure 28(a) is a photograph of typical plugs ready for installation. Figure 28(b) is a photomicrograph of a junction taken after the sleeve had been pressed off a completed unit.

The plugs were installed in bored holes in the beryllium dishes as the final machine operation. Each plug was pressed into place with a shrink fit so that the face of the sleeve was flush with the adjacent surface of the beryllium dish. The mandrel was then machined off and the core face was hand finished flush with the sleeve surface. It is estimated that the distance from the calorimeter face to the center of each thermocouple bead was known with an error less than ±0.05 mm after the final installation.

Electrical connections and check-out.- Inconel-sheathed duplex lead wire with aluminum-oxide insulation was used from the thermocouple plugs to the commutator system. The chromel-alumel lead wires were a nominal 0.075 mm diameter and the sheath was 0.46 mm in diameter. Welded connections were made at the terminals of the thermocouple plugs and soldered connections were made at the PDM commutator plugs. Thermistors were used to monitor the temperature of the commutator plugs which served as the cold junctions for the thermocouple measurements. The use of very small lead wire was dictated by the great number of thermocouples involved (222 in the forebody assembly). Breakage, particularly near the commutator plugs, was a continual problem. The condition of the lead wires was frequently monitored by resistance measurements during assembly operations, and repairs were made where possible. Connections at the commutators were made in 12 plugs of 44 pins each. To avoid disconnecting these plugs for thermocouple ring-out, the PDM system was adapted for use as an ohmmeter so that the thermocouples could be electrically checked out through the reentry-package telemetry

system. This use of the system is described in appendix D. Since the thermocouple junctions were grounded to the beryllium, the resistance of each lead, as well as the loop, could be measured. The measurements indicated a good electrical contact between the junction and the beryllium and an inferred good thermal contact.

Decisions concerning thermocouple lead repairs were predicated on a combination of accessibility and need to retain sufficient redundancy for the more important locations. The final check-out before Fire II indicated that 21 of the total of 144 thermocouples were inoperative because of opens or shorts which had not been feasible to repair. About an equal number of thermocouples failed or did not operate through the complete data period in flight. However, the degree of redundancy was such that the loss of these thermocouples did not restrict the analysis of the desired heating data.

Phenolic-asbestos installations.- Thermocouples were mounted in each of the phenolic-asbestos insulation layers for diagnostic purposes. The thermocouples were mounted in plugs similar in design to those in the beryllium calorimeters with the following differences: (1) phenolic-asbestos base material, (2) three junctions rather than four, (3) the forward two junctions and lead wires were platinum/platinum—10-percent-rhodium, (4) the thermocouple beads were phenolic bonded in place, and (5) the lead-wire insulation was teflon.

Afterbody Calorimeters

Heat-storage-type calorimeters were installed at 12 locations on the afterbody. A gold slug, mounted in aluminum silicate insulation, was the heat sink. Chromel-alumel thermocouple junctions (two for redundancy) were swaged into the back side of the gold slug to monitor its temperature. Reference 6 gives a more detailed description of the calorimeter and presents the data for Fire I.

FLIGHT PERFORMANCE

The performance of the reentry-package system for Fire II was excellent; other than the loss of some calorimeter thermocouples, there was no known malfunction of any instrumentation or operational element. The ejection of the phenolic-asbestos shields, the disabling of the tape-recorder erase-record heads, and the operation of the fail-over switch occurred at the expected times. Telemetry blackout (VHF) started at an altitude of about 102 km and ended when the velocity had decreased to about 3.6 km/sec at an altitude of about 32 km. Both the TLM-18 antenna system on Ascension Island and the backup ship provided good telemetry coverage in the terminal area. Four full cycles of the stored reentry data were acquired between the end of blackout and final loss of signal. Figure 29 is a reproduction of an oscillograph record of the reentry period data. This

particular record is from the fourth replay of the recorded data over the real-time link after the fail-over switch had operated. The arrangement of the channels on the record from top to bottom is the same as shown in figure 5. The display for the PDM channel is the direct PDM output and not a PAM (pulse amplitude modulation) conversion. Figure 30 is a larger scale reproduction of a section of a similar record showing the spectral radiometer trace at two different periods of the reentry.

The onboard-tape-recorder performance remained within the limits that allowed good tape-speed (wow and flutter) compensation of the received data. All channels were recovered without significant degradation due to noise. Each total-radiometer channel had random noise in the replayed data that ranged from nearly zero to as much as 0.2 V peak-to-peak; however, the noise frequency was very high compared to the data frequency and was adequately eliminated by fairing. The spectral-radiometer channel did not appear to suffer any noise addition due to the telemetry system.

CONCLUDING REMARKS

The flight-data requirements of Project Fire were successfully met by the reentry-package instrumentation system. Good performance was obtained from both the "off-the-shelf" and the specially developed instrumentation components.

The performance of the radiometer system was excellent with no evidence of any in-flight degradation. The probable accuracy of the total-radiometer measurements (at the instrument) is considered to be within about 20 percent of reading except for any additional error introduced by the known spectral-response variations. The probable accuracy of the spectral-radiometer measurements (at the instrument) is considered to be within about 25 percent of reading except for the amplitude of radiation bands narrower than the bandwidth of the radiometer.

The absolute calibration of thermal radiometers does not presently lend itself to a high degree of precision because of the number of factors involved and the indirect nature of many of the measurements required. The calibration cross-checks accomplished with the Fire II radiometers provided increased confidence in the validity of the calibrations. The use of every possible cross-check is strongly recommended to avoid the possibility of gross calibration errors.

A truly flat spectral response for a total radiometer over the wavelength range required for Project Fire is very difficult to obtain with available elements; even the degree of flatness is difficult to establish. The spectral characteristics of every optical element involved should be carefully examined both in the design and the calibration of the instrument.

The thermocouple installation technique provided an excellent method of mounting very small mass junctions at precisely known locations in the calorimeters. The apparently delicate installations proved to be very rugged in assembly and flight; the major breakage problem was in the area where the extension leads were terminated at the data system.

Langley Research Center,
National Aeronautics and Space Administration,
Langley Station, Hampton, Va., July 15, 1966.

APPENDIX A

SUMMARY OF FIRE I INSTRUMENTATION AND PERFORMANCE

The performance of the instrumentation system during Fire I was, in general, satisfactory but there was not a complete recovery of the reentry data because of an antenna problem. The flight test was further compromised by large body motions during reentry as discussed in reference 1. Fire II was conducted as a repeat test to confirm the Fire I data and successfully filled the gaps in the Fire I data. The significant areas in which there were problems or deficiencies during Fire I and changes which were made in equipment or procedures for Fire II are discussed in this appendix.

Antenna

At the time of spin-up, there was a partial failure of the delay-time antenna system. The character of the failure was indicative of a broken connection in the coaxial cable to the antenna and resulted in a loss of more than 20 dB in signal strength. During the subsequent replay of the reentry data, adequate signal was obtained only when the reentry-package attitude presented the higher gain lobes of the antenna pattern to the ground station. Generally, the usable periods were no more than 1 sec in duration and occurred at 2- or 3-sec intervals.

The original configuration of the fail-over switch shown in figure 6 was arranged to transpose the function of the two transmitters if a failure of the delay transmitter was detected by a power sensor in the antenna cable. The mismatch caused by the delay antenna failure apparently overloaded the delay transmitter to the point of final failure so that the fail-over switch operated to place delay modulation on the real-time transmitter. This occurred at about the time of loss of signal at Ascension Island but in range of a backup ship which recovered part of one cycle of replayed data before splash. Data for about two-thirds of the reentry period were recovered by merging the usable sections of data from the two receiving stations.

For Fire II, the antenna cabling was completely reworked by using stranded-center coaxial cable and better routing and tiedown. The fail-over switch function was also changed to provide redundant transmission of the reentry data.

Radiometer-System Electronics

The radiometer-system electronics were very difficult to prepare and maintain; however, the performance in flight was satisfactory. Each channel used dc amplifiers, with logarithmic compression at the input; adequate temperature compensation and stability were difficult to achieve. The total-radiometer channels had a dynamic range of

four decades and the spectral channel had a range of six decades; the logarithmic shaping was not adequately linear over these ranges and regions of very low resolution existed, particularly in the midrange of each channel. There were also problems in obtaining reliable operation of the power supplies and the cam-operated switches which provided the calibration functions; consequently, it was decided to replace the radiometer electronics completely for Fire II. At the same time, there was some reduction in the design ranges based on the data obtained in the first flight.

Total-Radiometer Calibration

The total radiometers were calibrated by using the same basic apparatus described in the body of this report except that the optical pyrometer was not used and the attenuating filters were perforated screens. A between-flight evaluation of the calibration procedures revealed rather large errors that had existed when the Fire I radiometers were calibrated. The two principal sources of error were a nonuniform calibration steradiancy and the geometry of the reference thermopile.

Referring to figure 17, the diameter of the lens was used as the exit pupil diameter in lieu of a stop such as S_2. Also, the field stop S_1 was not set to a diameter that blocked furnace wall rays out of the optical path. A survey with an adjustable stop adjacent to the lens showed that the steradiancy was very nonuniform across the full field defined by the lens diameter. From these measurements, the steradiancy within the acceptance field of the radiometer being calibrated was found to be some 40 percent greater than the average steradiancy determined with the lens diameter as the stop and used as the calibration value.

The reference thermopile was a standard laboratory type having a lamp-black receiver disk at the apex of a blackened conical entrance shield in a water-cooled housing. Absolute calibrations of this thermopile were made in the conventional manner by using a black body or a lamp at a standard distance. Such a source provided irradiance by essentially parallel rays that completely filled the entrance cone of the thermopile. Tests showed that nearly 25 percent of the energy reaching the receiver disk was reflected from the wall of the conical entrance cavity; however, when the thermopile was used in the radiometer calibration apparatus, it was irradiated by a converging bundle of rays which did not strike the conical entrance wall. This effectively lowered the sensitivity ($V/W\text{-}cm^2$) of the thermopile when used for the radiometer-source calibration compared with the sensitivity determined during the absolute calibration of the thermopile. As a result, the calibration-source steradiancy determinations had been low by nearly 25 percent since the thermopile sensitivity enters the computation as a reciprocal.

It should be noted that both of the error sources made the actual calibration steradiancy levels for the total radiometers higher than the measurements had indicated. To

confirm the product of these errors, a total radiometer was calibrated by using the original procedure and the modified procedure used for Fire II. A comparison of the two calibrations showed that any radiometer output voltage represented an input steradiancy that was about 75 percent greater than the steradiancy value determined when the Fire I calibration procedure was used. The data obtained during Fire I were subsequently corrected by the amount indicated by these tests.

Spectral-Radiometer Calibration

The spectral radiometer for Fire I was calibrated by using the monochromatic calibration apparatus previously described and shown in figure 20 except for differences in optical geometry and the reference thermopile; there was no cross-check calibration made by using the continuum source. The optical geometry of the calibration apparatus, as used at that time, provided a larger usable calibration field θ which much more nearly filled the radiometer acceptance field. The effects of the triangular distribution of irradiance over the length of the slit image were largely compensated by the geometry of the reference thermopile. The thermopile used in the Fire I calibration had a 0.75-mm-square receiver surface; since this surface was roughly twice as wide as the slit image, the thermopile gave an indication which was low for the region it was measuring but which was more nearly an average for the necessary image length. These two differences in the apparatus, to the extent they have been evaluated, indicate that a large part of the known error found in the apparatus during the Fire II calibrations (see page 20) was not present during the Fire I calibrations.

APPENDIX B

HEAT-SHIELD EJECTION SYSTEM

Heat shields were included in the layered forebody of the reentry package to protect the second and third calorimeters and the primary structure as indicated in figure 2. The forward two of these shields were arranged for command ejection to expose the second and third calorimeters at the proper times during reentry. The design of the shields had to meet the requirements of heat protection and of rapid ejection with minimum dynamic disturbance of the reentry package. The shield and ejection-system design also had to allow for a final assembly several months before launch.

Heat Shields

The heat shields were molded of a high-density phenolic asbestos, a material selection based on mechanical strength as well as heat-protection considerations. Figure 31 is a photograph, from the back side, of one set of the ejectable shields in an assembly test fixture. Each shield was molded in four quadrants. A tension link tied quadrants A and C together and a "jig-saw" configuration retained quadrants B and D. The mating edges of the quadrants were machined for an overlapping seal joint; the rim of the assembly was arranged to hook over the rim of the succeeding beryllium calorimeter dish. The numerous pads that can be seen were bearing points; each was covered with teflon to reduce the sliding friction on the beryllium during ejection. Two elliptical springs were mounted in the rim of each quadrant; at assembly, they were compressed to a preload of about 1000 N each to provide the ejection force. The tongue on quadrant A extended across the center line to provide material for mounting the stagnation radiometer window; the hole for the window had not been drilled when the photograph was made.

Ejection Link

The ejection link can be seen bolted to quadrant C in figure 31. Figure 32 is a photograph of an assembled link and a dismantled link. The structural parts of the link were made of a precipitation-hardening stainless steel. One end of the link was made with a slot and the other had a mating tongue. When these parts were mated, they were locked by the two wedge-shaped detents which were positioned by the keepers. This assembly was tension wrapped with a stranded exothermic fuse wire made of aluminum with a palladium jacket. When this wire was heated to the melting point of the aluminum, an exothermic alloying action took place and the wire immediately disintegrated. This action freed the detents and allowed the link ends to separate.

APPENDIX B

Ignition Circuit

Ignition of the fuse-wire action was accomplished electrically with a dual-igniter system for redundancy. Two short loops of fuse wire were inserted under the load-bearing wrap of wire and brought out as lead wires. One end of each lead was reduced to a single strand to provide an electrical "hot spot" as an igniter when current was passed through the loop. The exothermic action started at the igniter, propagated along the fuse wire, and was thermally transferred to the load-bearing wrap. The igniter was designed for a 1.0 A "no fire" to meet range safety requirements; the "sure fire" current was about 3.0 A. A dual silver-zinc battery was used for redundant firing of the igniters through silicon-controlled rectifier (SCR) switches which were initiated by the reentry timer as indicated in figure 7. In the event that the preceding beryllium layer had not melted, because of trajectory or other anomalies, a circuit was arranged to hold off the timer command until beryllium melt was indicated. For this, two "break-wires" were inserted in one quadrant of each ejectable layer. Two plugs of opaque silica were set into the phenolic asbestos; a length of platinum wire, fed through holes in the silica, was exposed on the front face as the break-wire. The two break-wires in series provided a ground return which disabled the ejection switching system. Any momentary opening of either break-wire after beryllium melt gated an SCR memory circuit which then permitted completion of the normal timer firing circuit. Two identical circuits were used, one for each shield. When the shield ejection SCR was fired, a transistor switch simultaneously commanded the appropriate PDM commutator transfer.

Performance

The tension loading on the link at assembly was about 6000 N. The actuation time from current application was about 400 msec in tests. Wind-tunnel tests, under simulated dynamic-pressure conditions, indicated a time from first motion to full clearance of the package of about 20 msec. The flight performance of the system was excellent for both flights with rapid ejections and no significant disturbance in either case. The data indicate that during Fire II, the break-wire circuit did hold off the second shield ejection for a few msec after the programed time.

APPENDIX C

REFERENCE-DETECTOR CALIBRATION AND READOUT

During the calibration of the radiometers a total-irradiance measurement was required in the determination of the absolute total steradiancy of the calibration source. The detector used for this measurement was the same as the gold-black thermopile used in the total radiometers except that the seal window was barium fluoride rather than quartz. This detector was mounted in a water-cooled housing and can be seen in place in figure 16.

The absolute calibration of this detector is of primary importance since the absolute steradiancy determinations for the radiometer calibration depended directly on the absolute accuracy of the reference detector. Initially, calibrations were made with both a 1273° K black body and carbon-filament lamps used as the sources of absolute irradiance. A disagreement between calibrations made when these sources were used was traced to a change in characteristics of the carbon-filament "standard" lamps. Aside from this, there was the problem that either source provided very low absolute levels of irradiance (about 2×10^{-4} W/cm^2) compared with the levels at which the reference detector would be used (up to about 0.5 W/cm^2). Also, the spectral distribution of these sources was considerably shifted from that to be measured in the radiometer calibrations. These deficiencies would place an extreme dependence on the linearity and spectral flatness of the detector.

On the recommendation of the National Bureau of Standards Photometry and Radiometry Laboratory, a 1000-W tungsten-filament projection lamp was procured for use as a detector calibration source. An absolute calibration of this lamp, made at National Bureau of Standards, showed an absolute irradiance, at 1 m, of 8340×10^{-6} W/cm^2. At the same time, the contractor had a laboratory thermopile (lampblack receiver) calibrated by National Bureau of Standards and cross-checked against the calibrated projection lamp.

The color temperature of this lamp filament was about 3100° K which provided a spectral distribution very near that of the radiometer calibration source; however, it was known that an appreciable part of the total energy emitted by the lamp originated from the hot glass envelope at infrared wavelengths. Since the response of the reference detector might not be flat at these wavelengths because of the detector seal window, steps were taken to eliminate the lamp-envelope emission as much as possible. The lamp was first set up by the contractor with the recommended baffles and the calibrated irradiance at 1 m was confirmed with the laboratory detector which had been calibrated at National Bureau of Standards. A water-cooled baffle with a 17-mm aperture, which slightly

vignetted the filament area, was then permanently mounted in front of the lamp. The resulting calibration irradiance at a distance of 1 m was 60×10^{-4} W/cm^2 which was then used as the absolute standard of irradiance for reference-detector calibrations.

Several calibrations of the reference detector were made during the course of the radiometer calibration. The scatter of these calibration values was no more than ±2 percent, and the average sensitivity for the reference detector was 0.018 V/W-cm^2. The spectral flatness of this detector was checked by the same method used for the radiometer detectors.

A null-balance readout system was used with the reference detector for its calibration and for its use during radiometer source calibrations. A 0- to 100-V dc power supply, monitored by a digital voltmeter, was connected across a voltage divider of precision resistors consisting of a 1-MΩ resistor and a 1-, 10-, or 100-Ω resistor as required. The low end of the divider, which had voltage ranges of 0 to 100×10^{-6}, $\times 10^{-5}$, or $\times 10^{-4}$ V, was connected to balance the thermopile output voltage, the null being detected with a spotlight galvanometer in the circuit. The system provided good resolution and repeatability in the range of use (roughly 10 to 10 000 μV) and had the advantage of measuring the thermopile output at a zero-current condition.

APPENDIX D

CALORIMETER THERMOCOUPLE CHECK-OUT

The forebody calorimeters and heat shields of the reentry package had a total of 222 thermocouple junctions installed. As the small-gage lead wires were installed and routed, frequent condition monitoring was necessary to detect breaks and indicate the need for repairs. Up to the point of connecting the thermocouple leads to the PDM commutator system, an ohmmeter was used to measure the loop resistance for each thermocouple as well as the resistance of the individual leads in the case of the grounded junctions in the beryllium dishes. A modification was incorporated in the PDM system so that it could be used as an ohmmeter for thermocouple ring-out without having to disconnect the small connectors and disturb the lead bundles.

Two leads from the amplifier input terminals were brought out of the PDM system case as indicated in figure 33. The test circuit shown consisted of an essentially constant current source and two switches S_1 and S_2. As the commutator sampled a thermocouple, the voltage across it was proportional to its resistance, and the PDM output was thus a measure of the thermocouple resistance. The loop resistance of the thermocouples ranged from about 20 to 400 Ω. The constant current source was set at 0.1 mA so that the 50-mV range of the PDM system represented 500 Ω full scale.

A data run was first made with S_1 open to measure any tare voltages present on the thermocouple leads. A data run with S_1 closed was then made as a measure of the total loop resistance for each pair of thermocouple leads. Further runs with S_2 in the A and B positions provided a measure of the resistance of each lead from the grounded-junction thermocouples. The commutator selector was commanded to connect each of the three commutators to the system in sequence for these same measurements. The test time for a complete set of measurements was only a few minutes. The data reduction was normally done manually from a high-speed oscillograph record of a PAM conversion of the PDM wave train. A shorted thermocouple would show a zero or very low reading, depending on where the short had occurred. An abnormally high resistance or open circuit would be indicated by full-scale limiting of the PDM system.

These measurements proved very useful in monitoring the condition of the thermocouples and leads during the preflight operations. In many cases, the measurements gave enough indication of the nature and location of defects that the repair operations were simplified. After the final use of the test circuit, the leads from the amplifier were carefully insulated and stowed.

REFERENCES

1. Scallion, William I.; and Lewis, John H., Jr.: Flight Parameters and Vehicle Performance for Project Fire Flight 1, Launched April 14, 1964. NASA TN D-2996, 1965.

2. Cauchon, Dona L.: Project Fire Flight 1 Radiative Heating Experiment. NASA TM X-1222, 1966.

3. Kelly, Francis J.; and Moore, Dwight G.: A Test of Analytical Expressions for the Thermal Emissivity of Shallow Cylindrical Cavities. Appl. Opt., vol. 4, no. 1, Jan. 1965, pp. 31-40.

4. Hass, G.; and Waylonis, J. E.: Optical Constants and Reflectance and Transmittance of Evaporated Aluminum in the Visible and Ultraviolet. J. Opt. Soc. Am., vol. 51, no. 7, July 1961, pp. 719-722.

5. Cornette, Elden S.: Forebody Temperatures and Total Heating Rates Measured During Project Fire 1 Reentry at 38 000 Feet Per Second. NASA TM X-1120, 1965.

6. Slocumb, Travis H., Jr.: Project Fire Flight 1 Heating and Pressure Measurements on the Reentry-Vehicle Afterbody at a Velocity of 38 000 Feet Per Second. NASA TM X-1178, 1965.

TABLE I.- REENTRY-PACKAGE MEASUREMENTS

(a) Primary-experiment measurements

Parameter	Instrument	Location or axis	Range
Radiative heating	Total radiometers (3)	Stagnation Offset Afterbody	0.1 to 100 W/cm^2-sr
	Spectral radiometer	Stagnation	0.1 to 100 W/cm^2-sr-μ 0.3 to 0.6 μ scan
Total heating: Forebody	Thermocouples in beryllium dishes	4 depths at 12 locations in each of 3 calorimeters	1500^{o} K
Afterbody	Thermocouples in insulated gold slugs	3 rays of 4 each in afterbody wall	1300^{o} K
Body motions	Accelerometers (5)	Longitudinal Longitudinal Longitudinal Transverse Normal	±6g 0 + 45g 0 - 120g ±6g ±6g
	Rate gyros (3)	Roll Yaw Pitch	0 to 24.5 rad/sec ±7 rad/sec ±7 rad/sec
Static pressure	Heated thermopile transducer	Orifice in afterbody wall	0 to 1330 N/m^2 absolute (0 to 10 mm Hg)
Radio attenuation	Directional couplers (2)	Each VHF antenna cable	0 to 4.5 W incident and reverse power

TABLE I.- REENTRY-PACKAGE MEASUREMENTS - Concluded

(b) Supporting measurements

EVENTS:

- Reentry-package separation
- Beacon antenna switchover
- -10g switch closure
- First heat-shield eject signal
- Second heat-shield eject signal

DIAGNOSTICS:

- Internal pressure
- Instrumentation system voltage
- Beacon transponder voltage
- Tape-recorder current
- Radiometer system voltages (4)
- Insulation-layer temperatures
- Afterbody structural temperatures
- Component temperatures

TABLE II.- SPECTRAL AND TOTAL TRANSMITTANCE OF FILTERS USED DURING RADIOMETER CALIBRATION

Wavelength, microns	Decimal transmittance for nominal percentage transmittance of –									
	80	60	50	40	30	20-1	20-2	10	5	1
[a]0.2536	0.724	0.554	0.486	0.387	0.261	0.166	0.163	0.079	0.074	0.0038
[a].3125	.764	.593	.522	.411	.306	.202	.206	.107	.060	.0082
[a].365	.778	.607	.550	.412	.335	.213	.216	.114	.058	.0098
[a].404	.786	.625	.550	.408	.338	.213	.213	.112	.057	.0098
[a].435	.790	.617	.549	.405	.332	.207	.212	.110	.057	.0100
[a].546	.793	.623	.539	.398	.316	.198	.200	.105	.054	.0100
[a].576	.795	.627	.537	.398	.313	.198	.200	.105	.055	.0104
.70	.799	.635	.536	.418	.310	.202	.205	.114		
.90	.808	.650	.528	.427	.301	.204	.204	.119		
1.10	.817	.660	.528	.435	.298	.203	.204	.122		
1.30	.826	.672	.519	.440	.289	.200	.199	.122		
1.50	.831	.678	.510	.442	.280	.191	.193	.122		
1.70	.834	.679	.502	.442	.269	.181	.187	.120		
1.90	.838	.682	.494	.443	.259	.174	.180	.106		
2.10	.839	.682	.483	.442	.248	.168	.171	.099		
2.30	.834	.677	.467	.438	.234	.161	.162	.110		
[b]Furnace continuum	0.815	0.664	0.495	0.426	0.253	0.186	0.186	0.110	0.062	0.0128

[a]Transmittances used for spectral-radiometer calibrations.

[b]Transmittances used for total-radiometer calibrations.

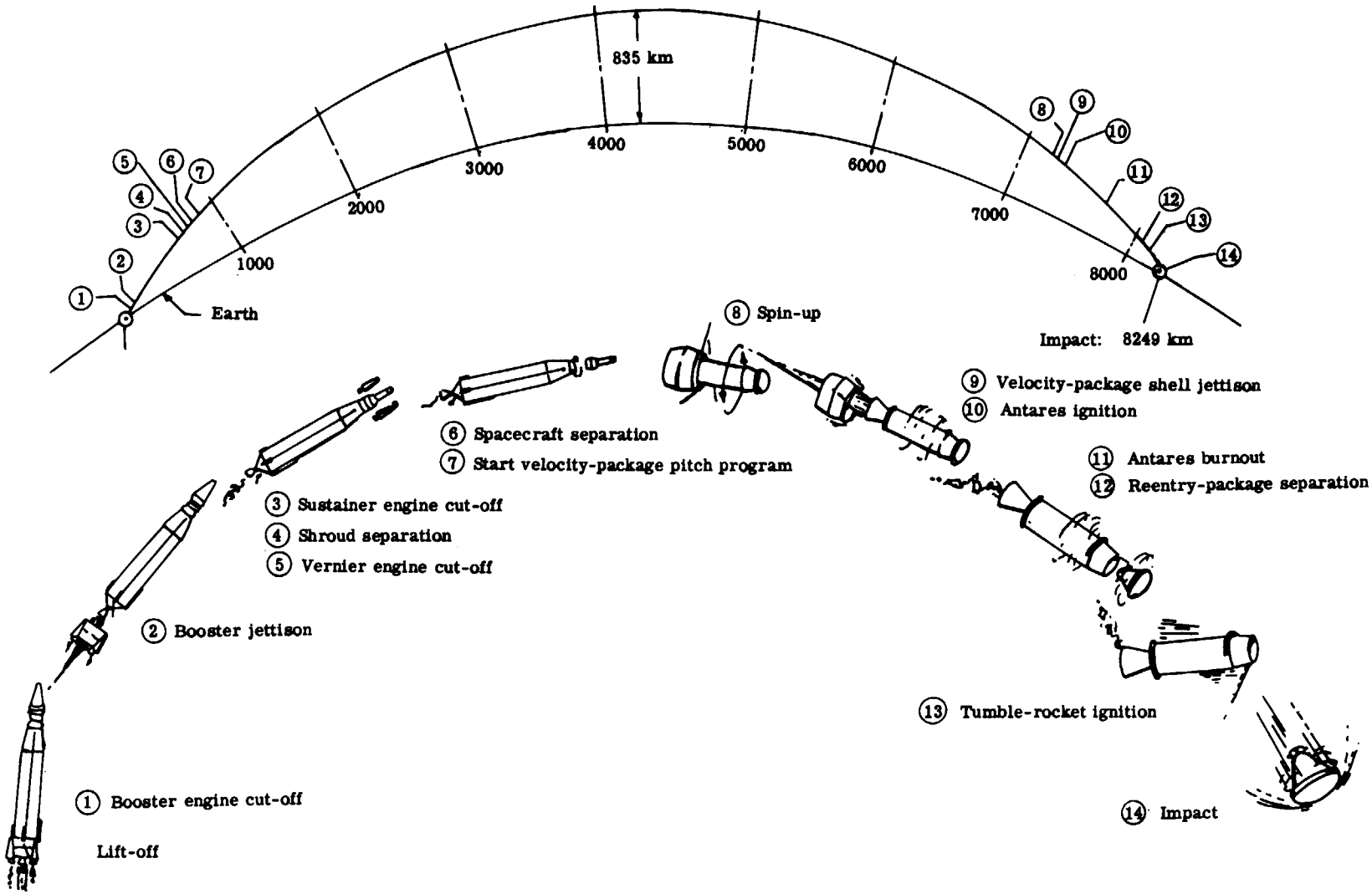

Figure 1.- Project Fire flight plan and sequence of events.

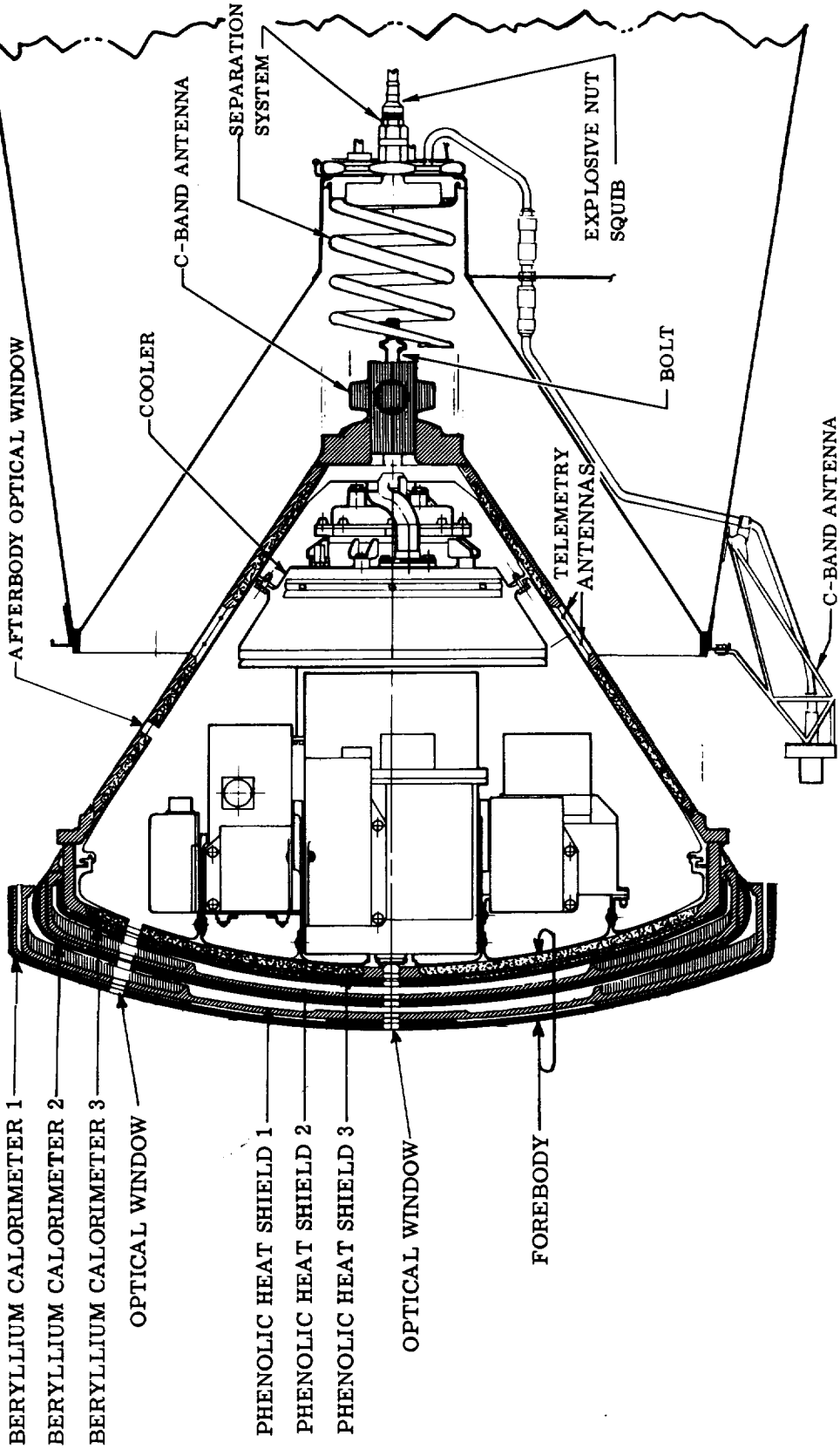

Figure 2.- Sectional view of reentry package and adapter.

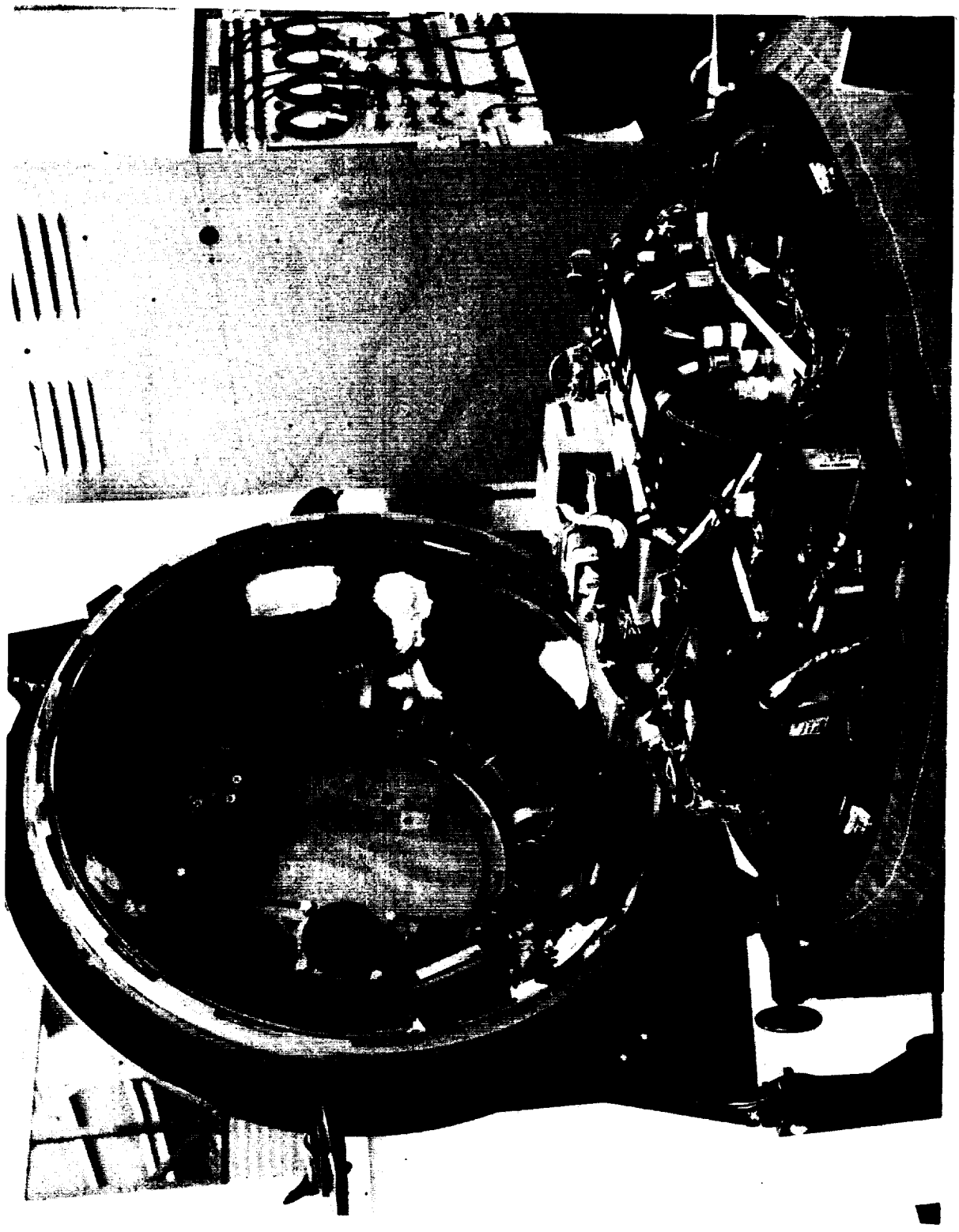

L-66-4449

Figure 3.- Opened reentry package in handling fixture.

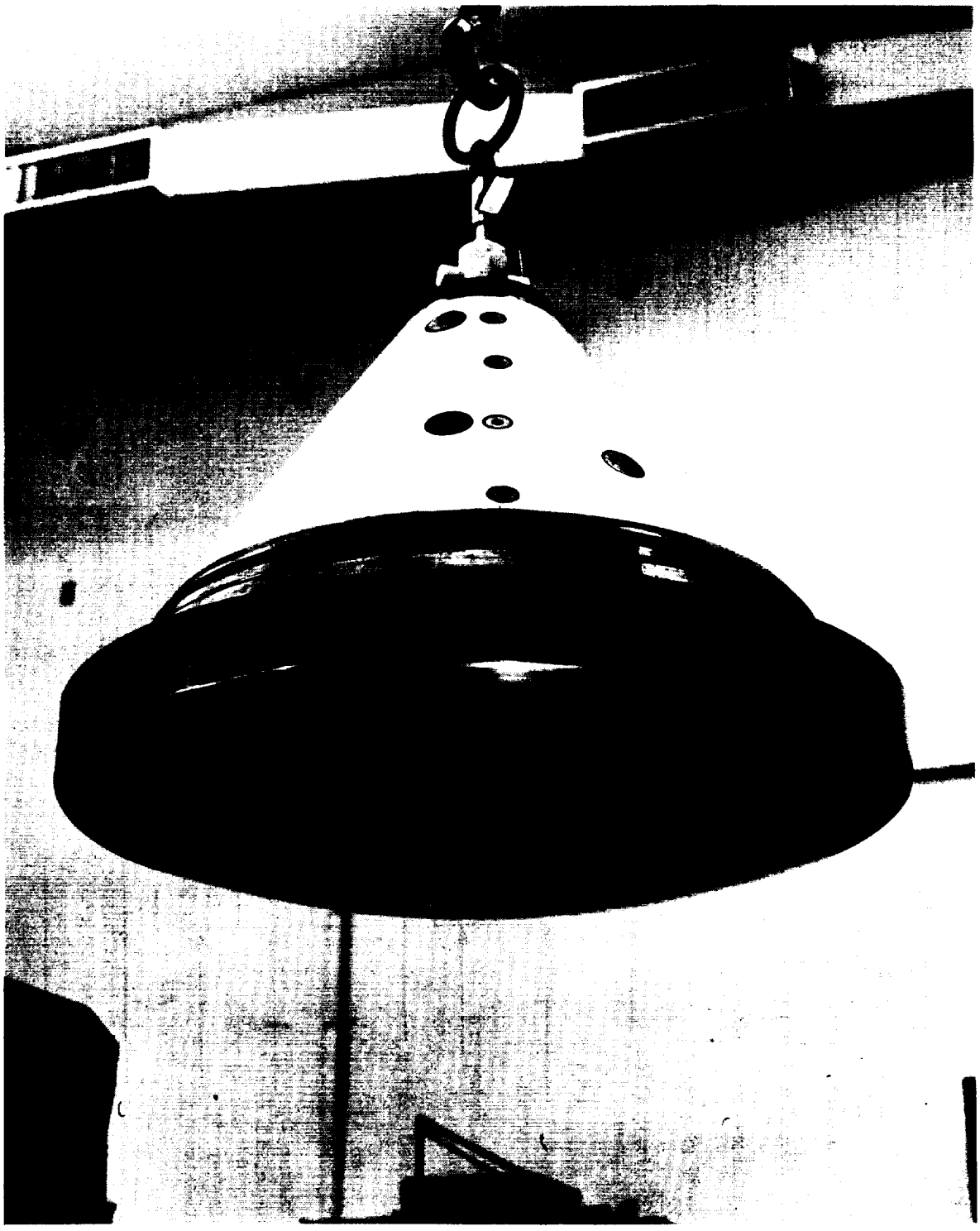

Figure 4.- Closed reentry package.

L-66-4450

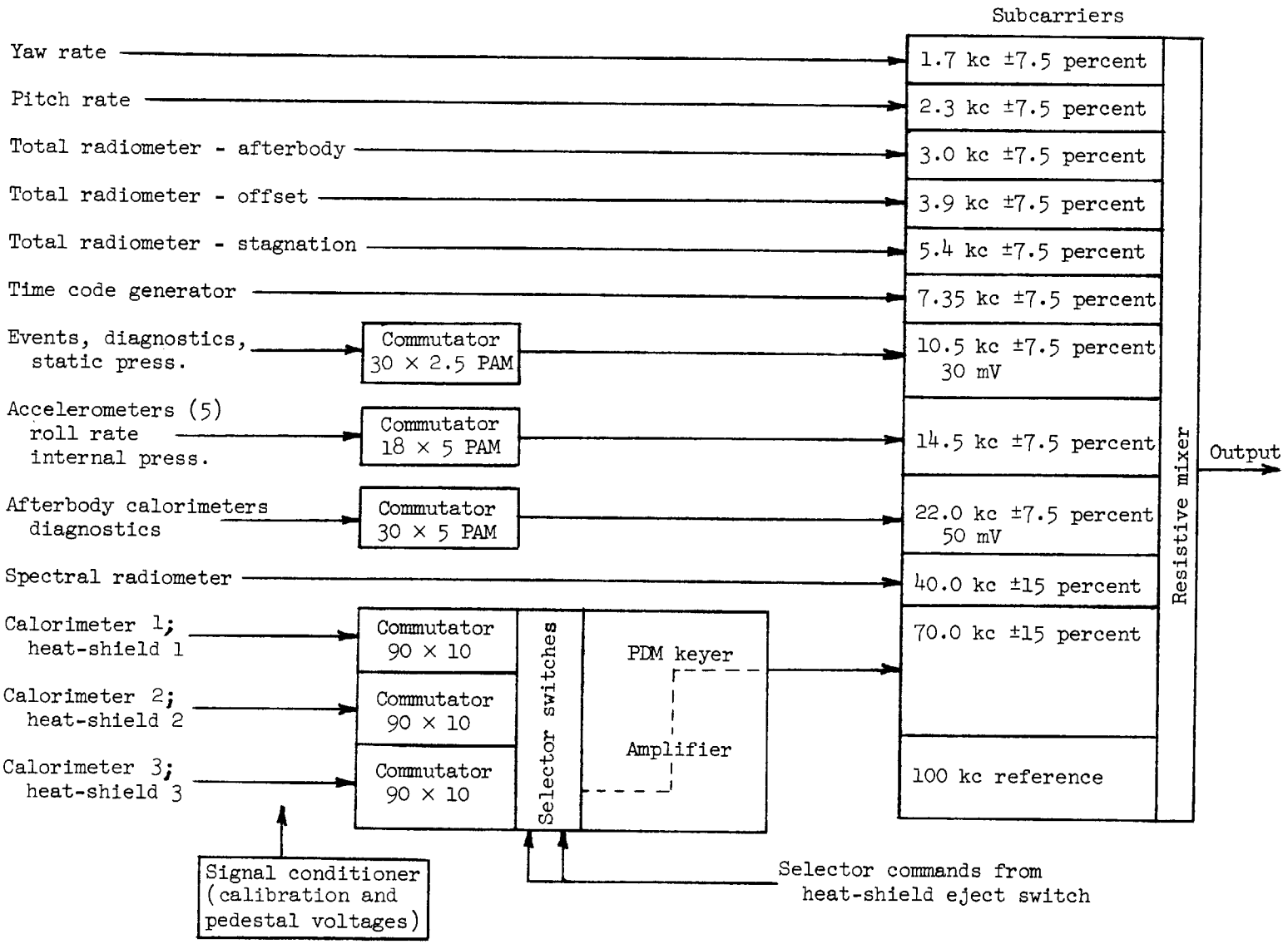

Figure 5.- Data acquisition system.

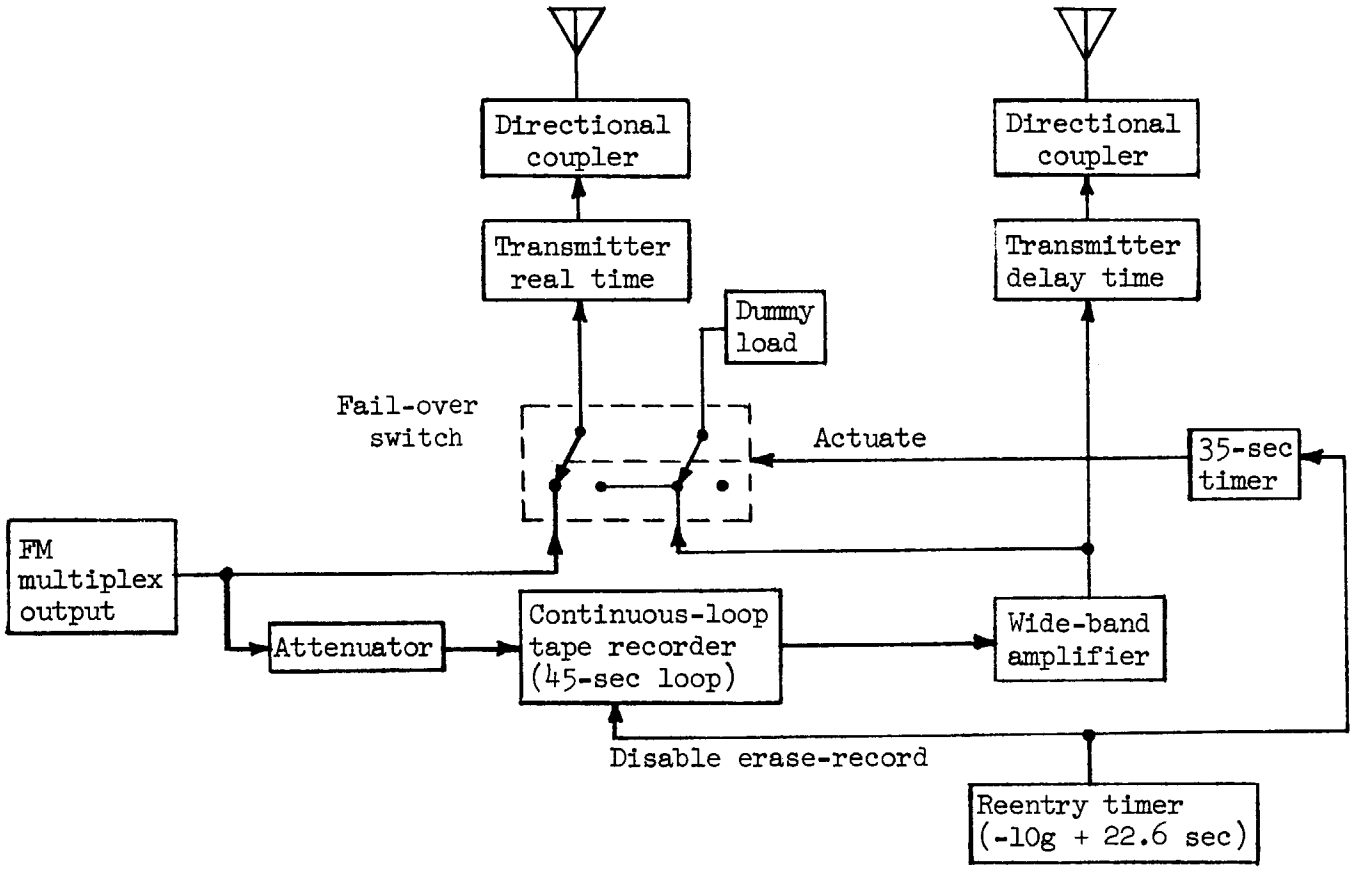

Figure 6.- Communications system.

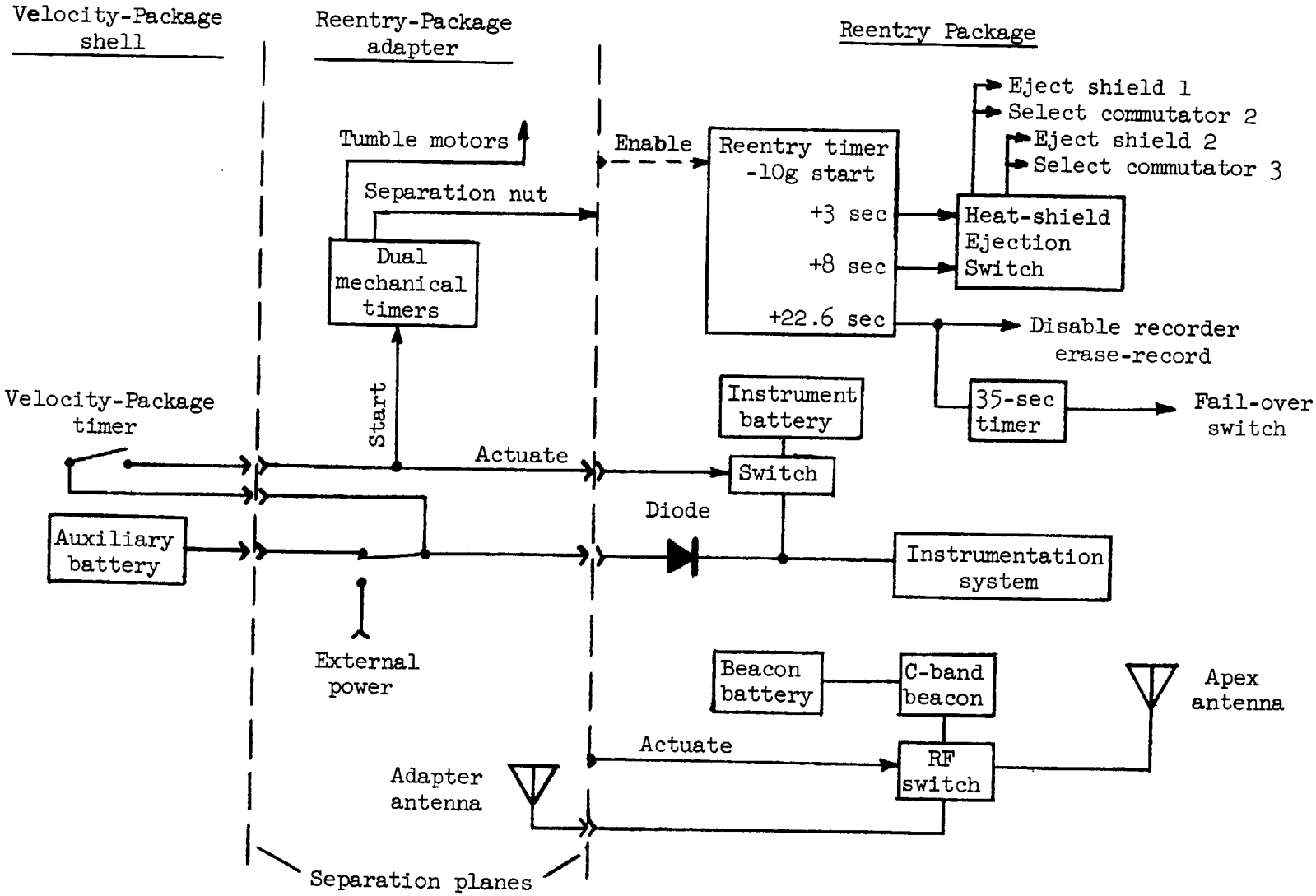

Figure 7.- Functional diagram of reentry-package sequence-of-events operation, instrumentation power, and tracking beacon system.

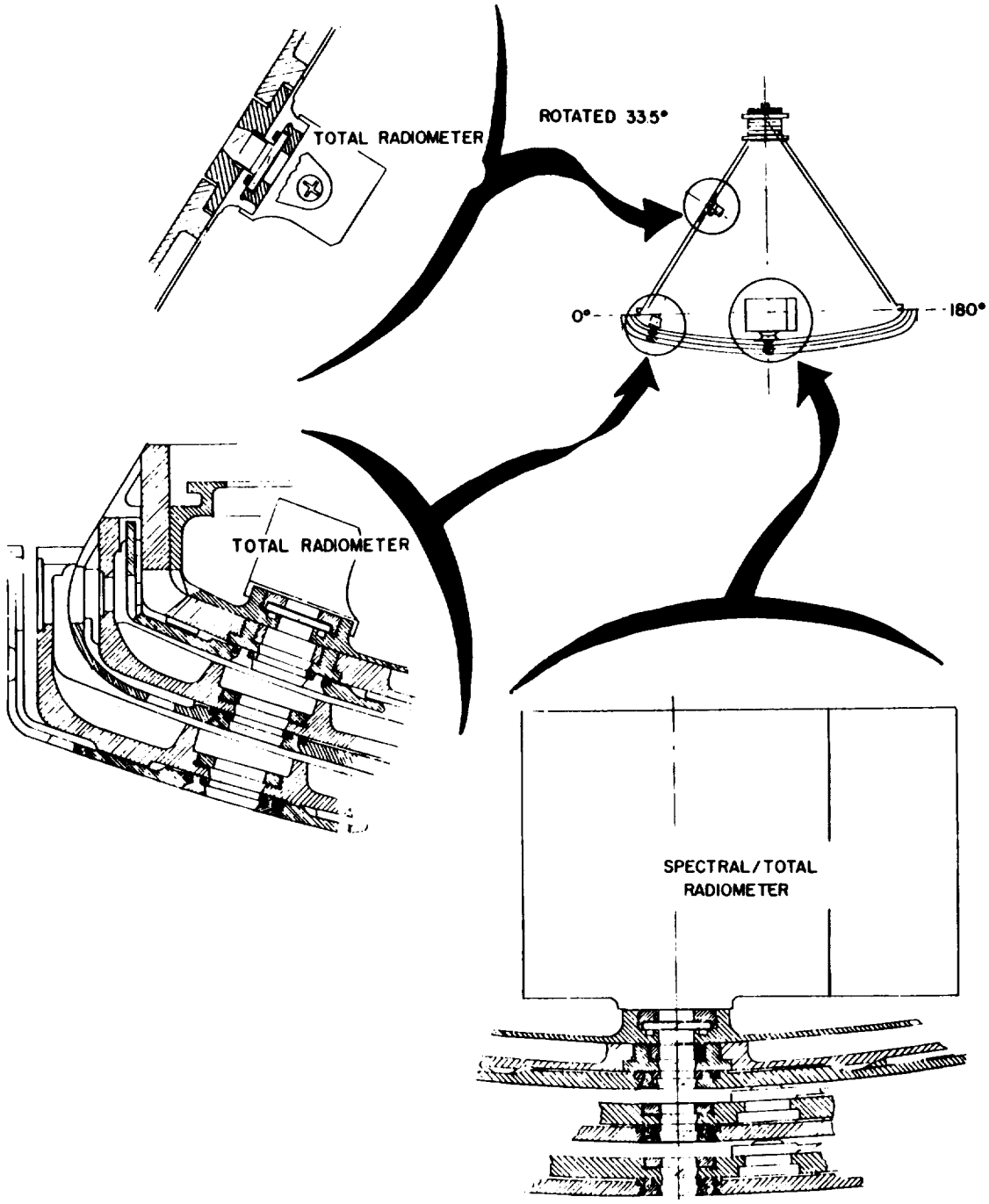

Figure 8.- Radiometer and window installations.

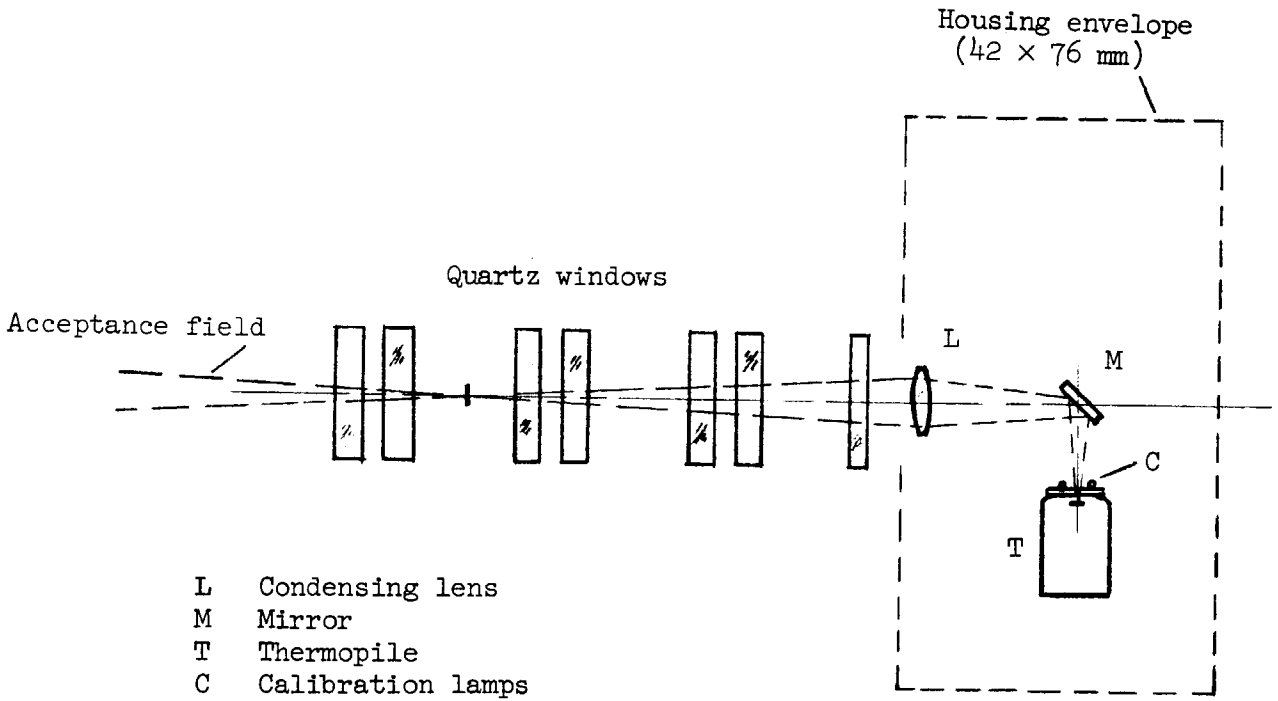

Figure 9.- Optical schematic of offset total radiometer.

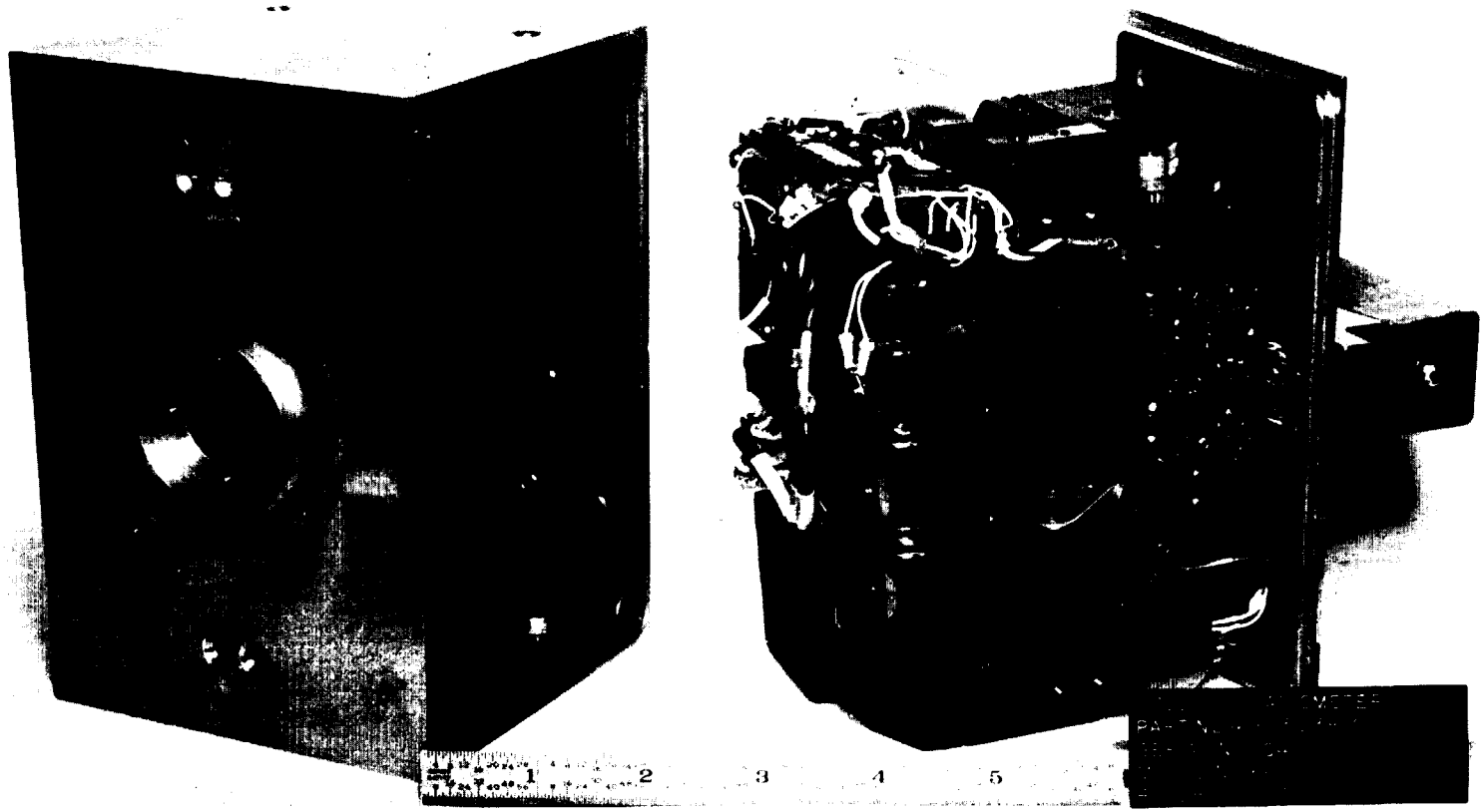

Figure 10.- Spectral total radiometer removed from case.

L-66-4451

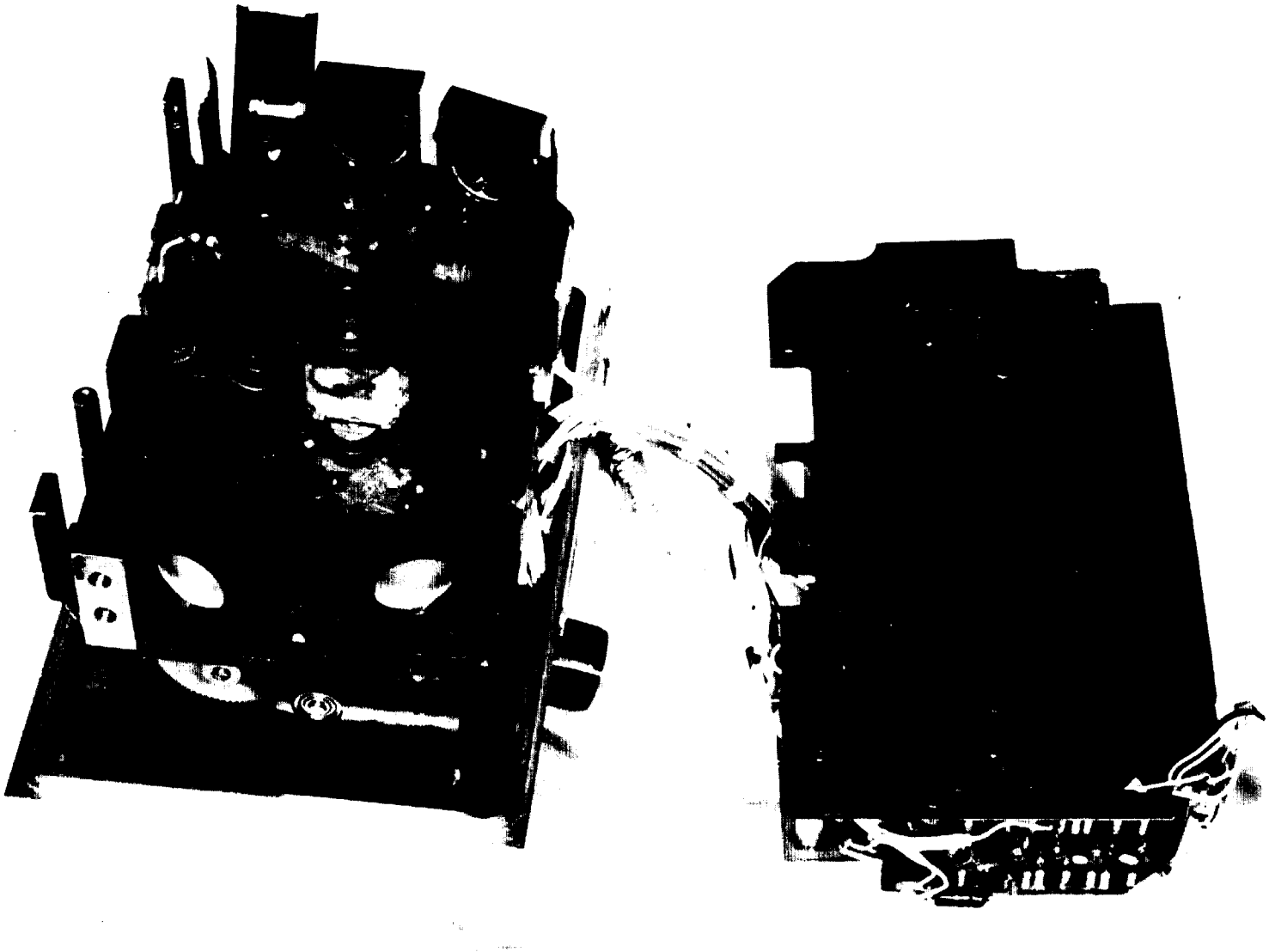

Figure 11.- Spectral total radiometer opened to expose optical deck.

L-66-4452

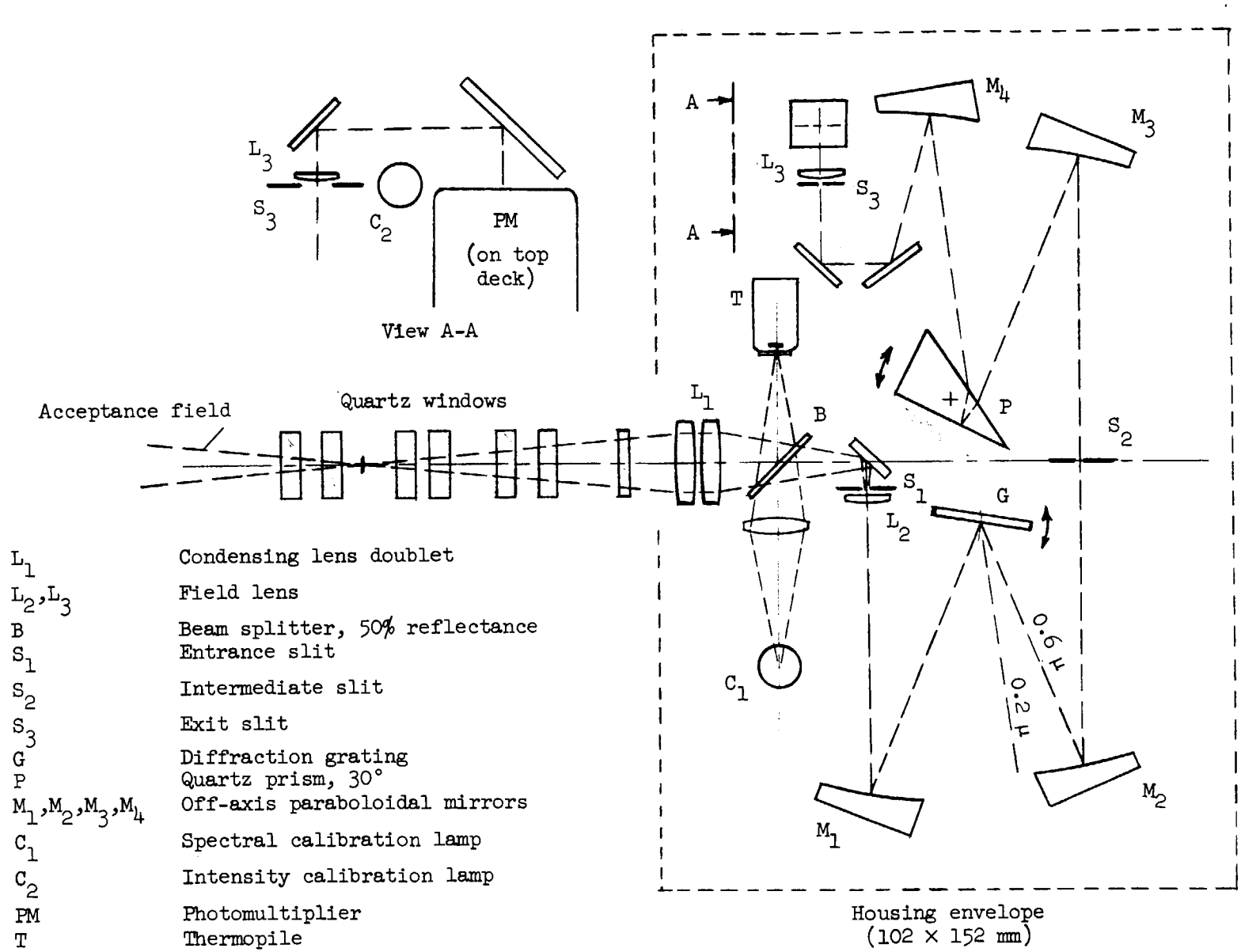

Figure 12.- Optical schematic of spectral/total radiometer. All unidentified reflecting surfaces are evaporated aluminum on quartz substrate.

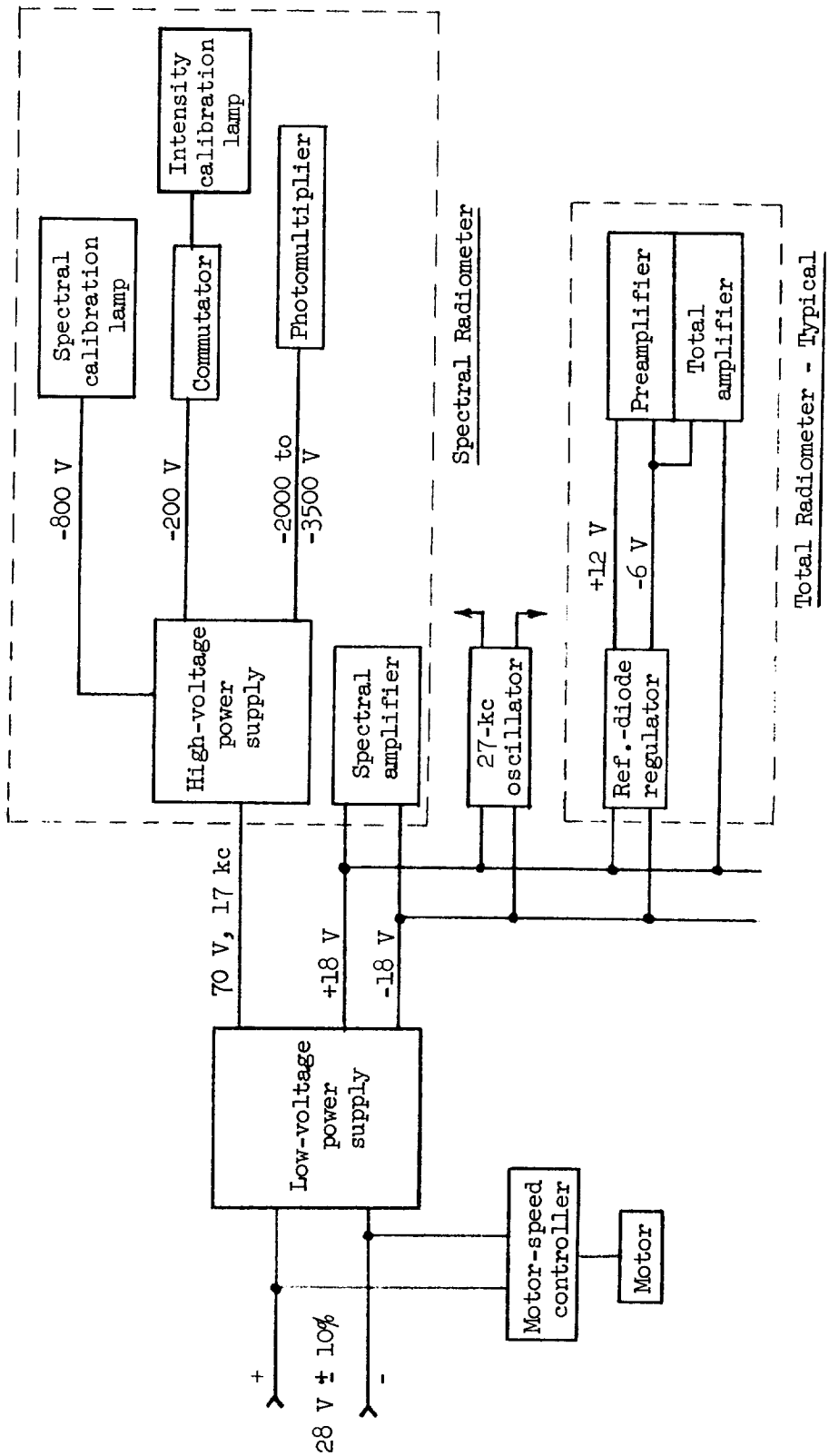

Figure 13.- Radiometer power-distribution block diagram.

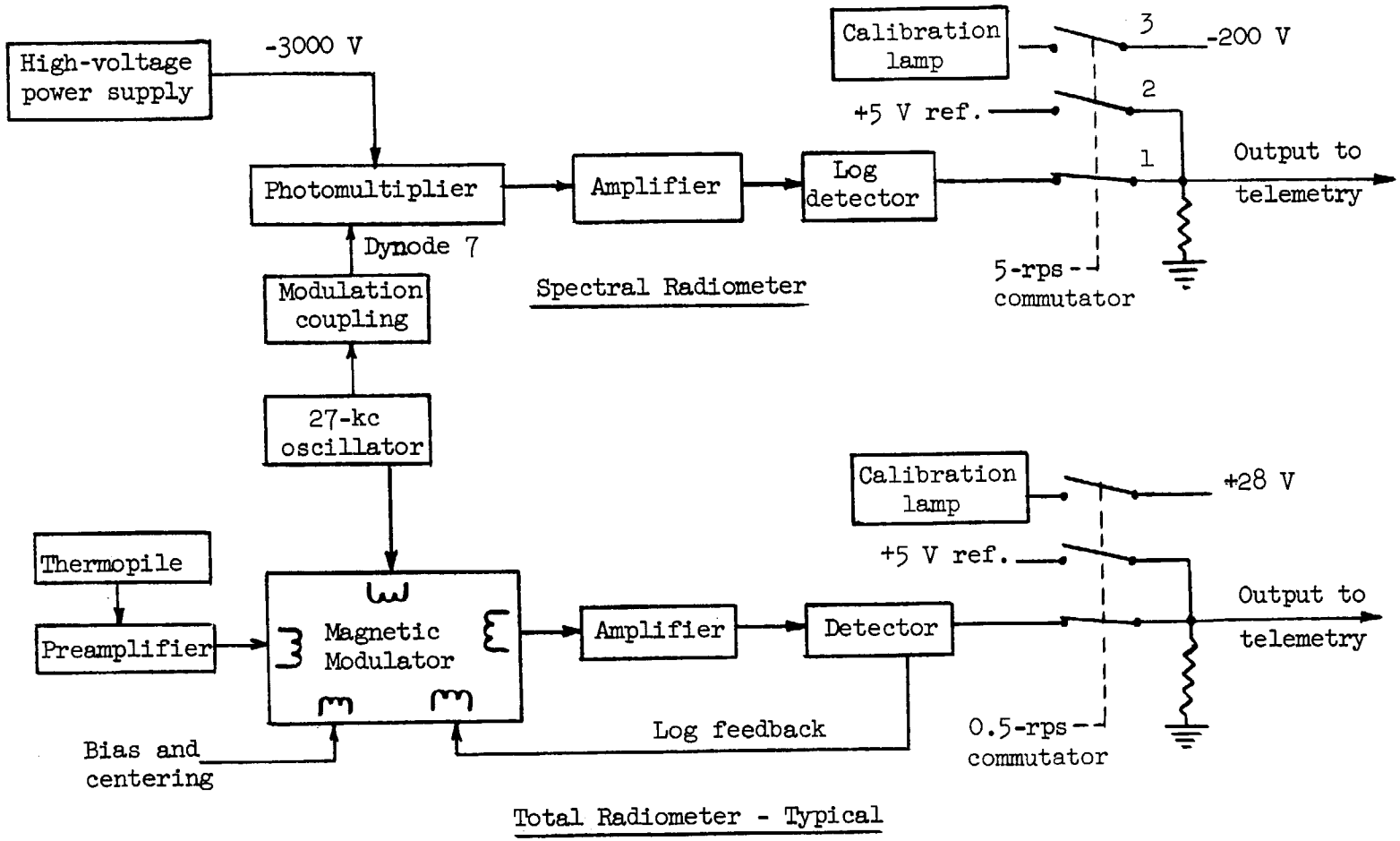

Figure 14.- Radiometer signal circuits block diagram.

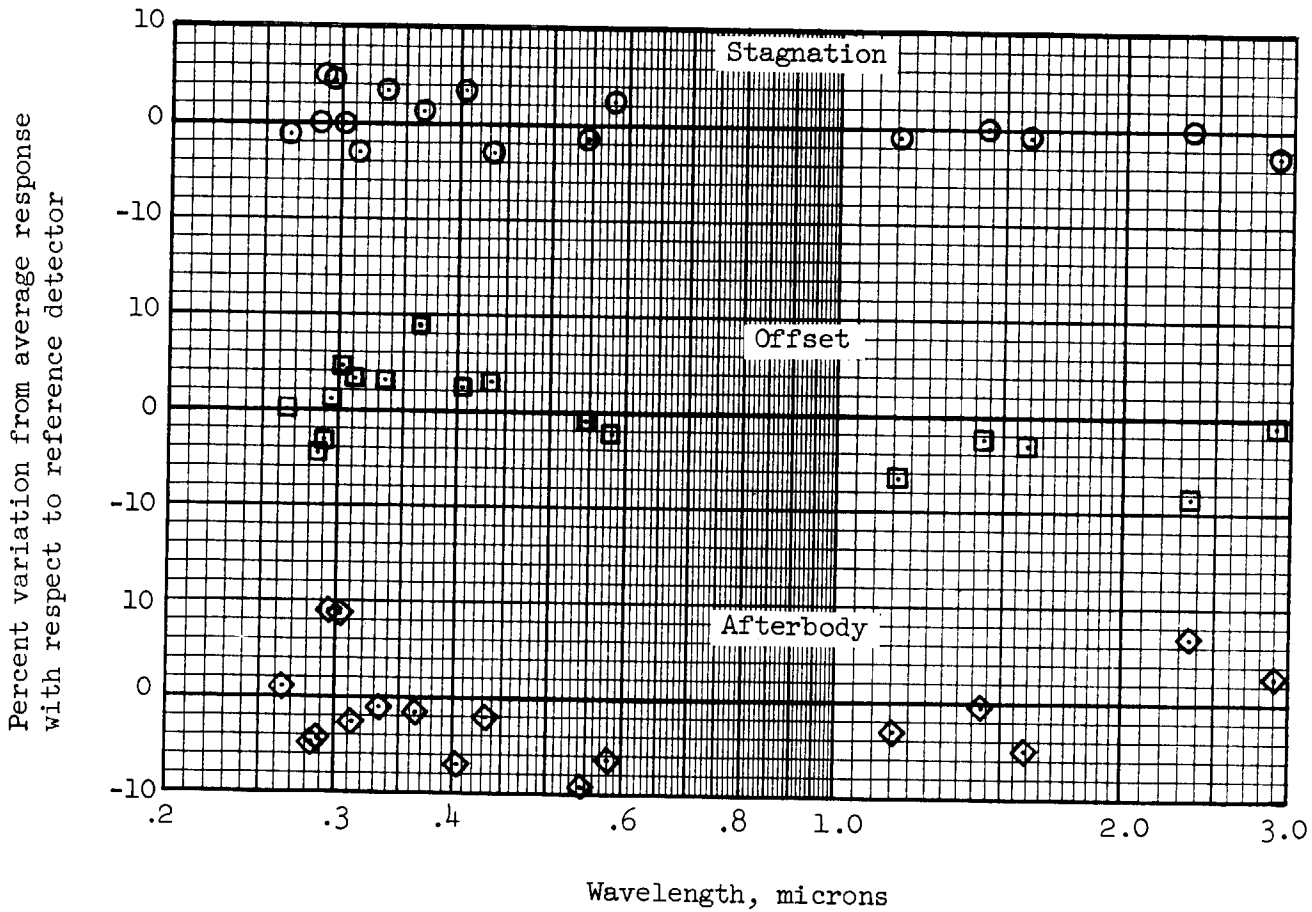

Figure 15.- Relative spectral response of detectors for Fire II total radiometers.

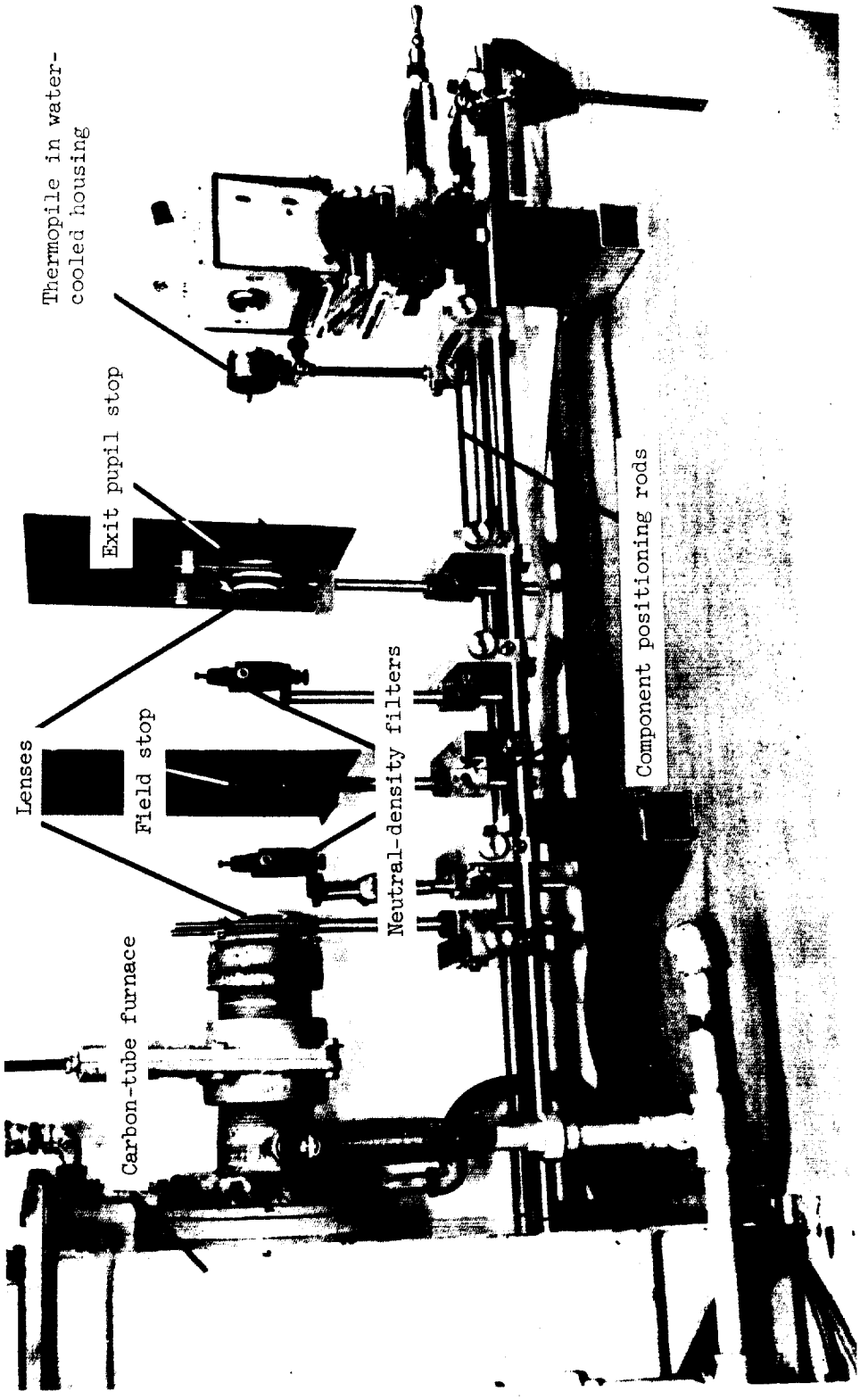

Figure 16.- Furnace calibration apparatus.

L-66-4453

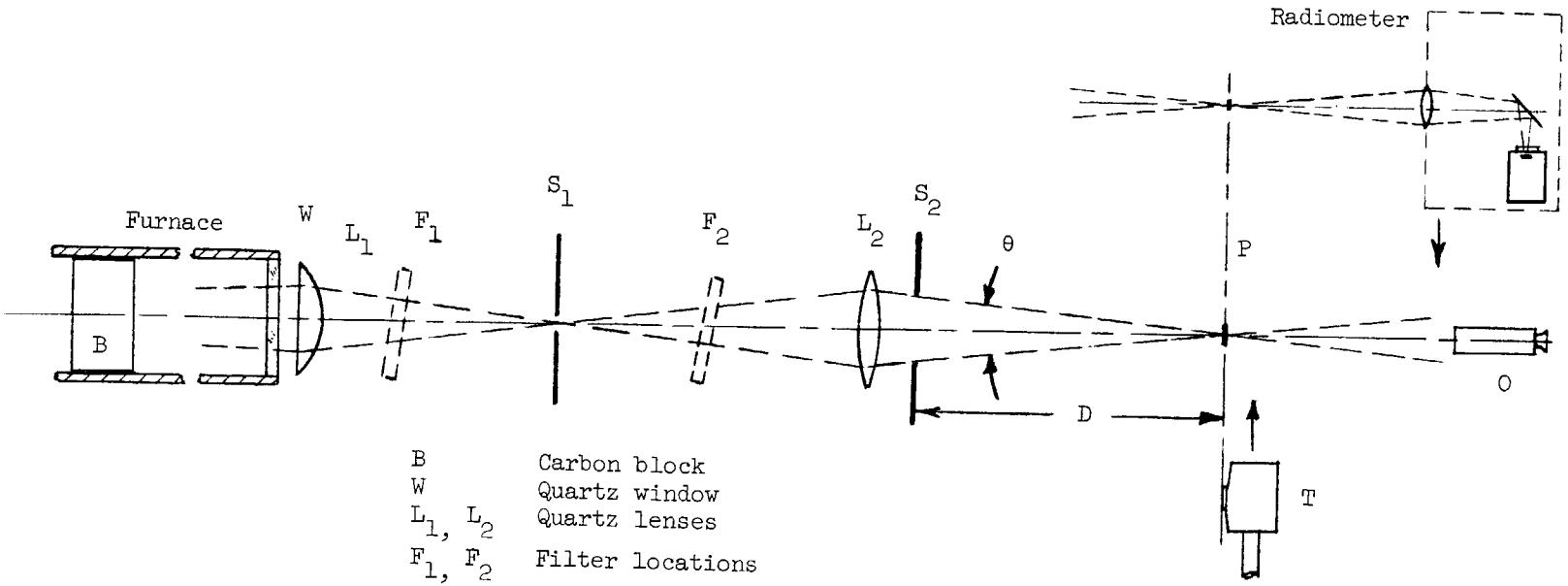

B	Carbon block
W	Quartz window
L_1, L_2	Quartz lenses
F_1, F_2	Filter locations
S_1	Field stop
S_2	Exit pupil stop
T	Reference thermopile
O	Optical pyrometer
P	Image plane
θ	Conical calibration field

Figure 17.- Schematic of furnace (continuum) calibration apparatus.

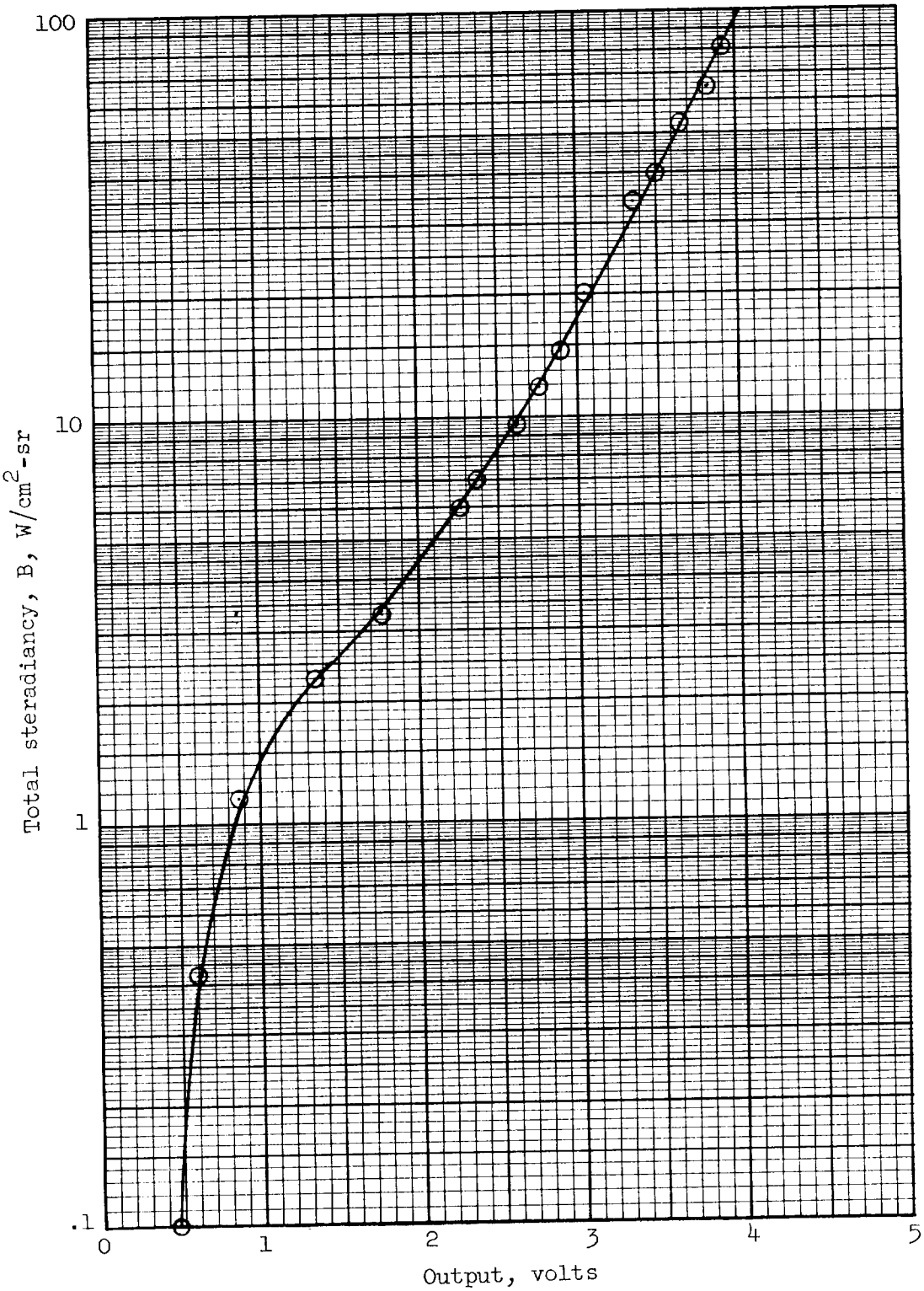

Figure 18.- Calibration of stagnation total radiometer.

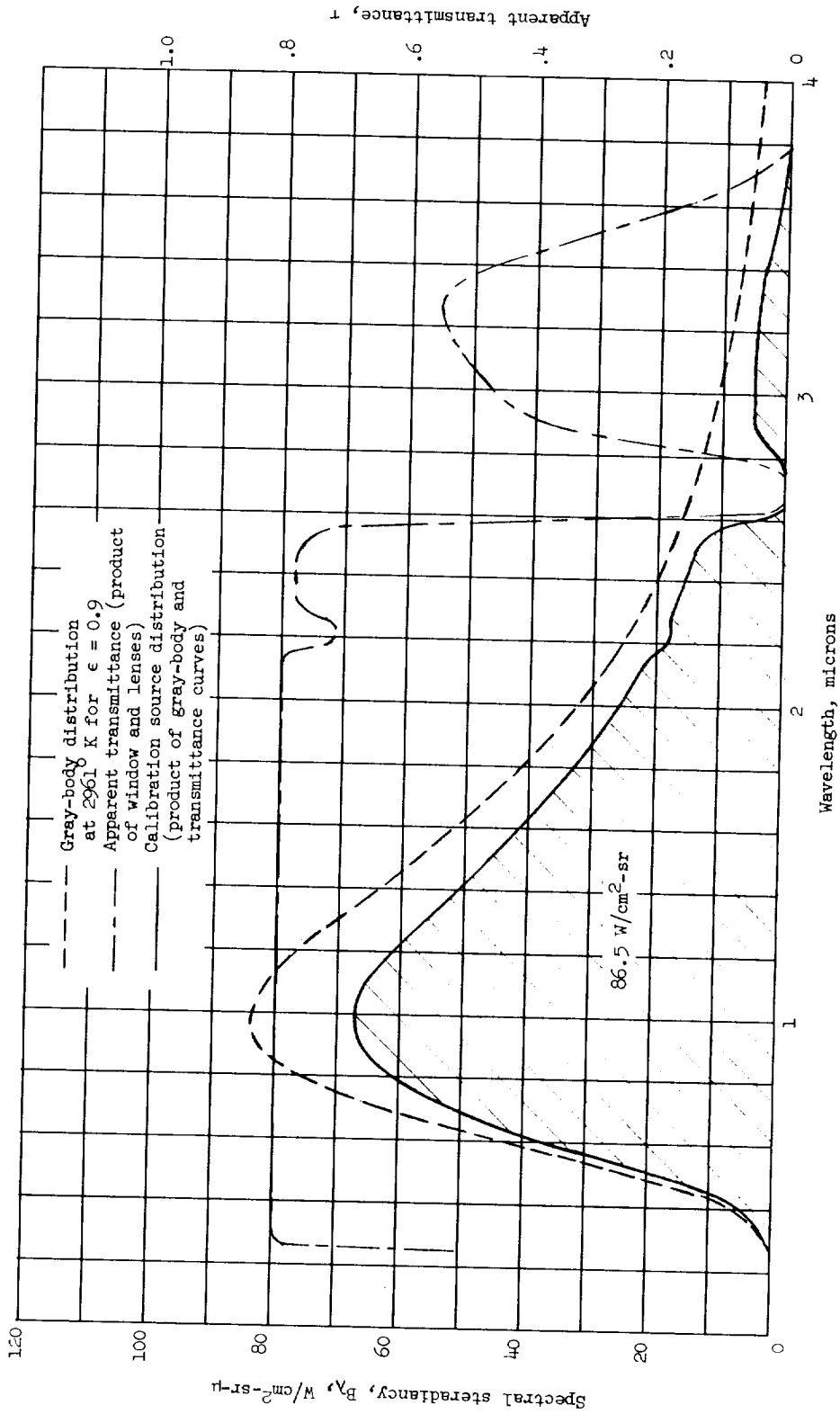

Figure 19.- Spectral steradiancy of continuum calibration source.

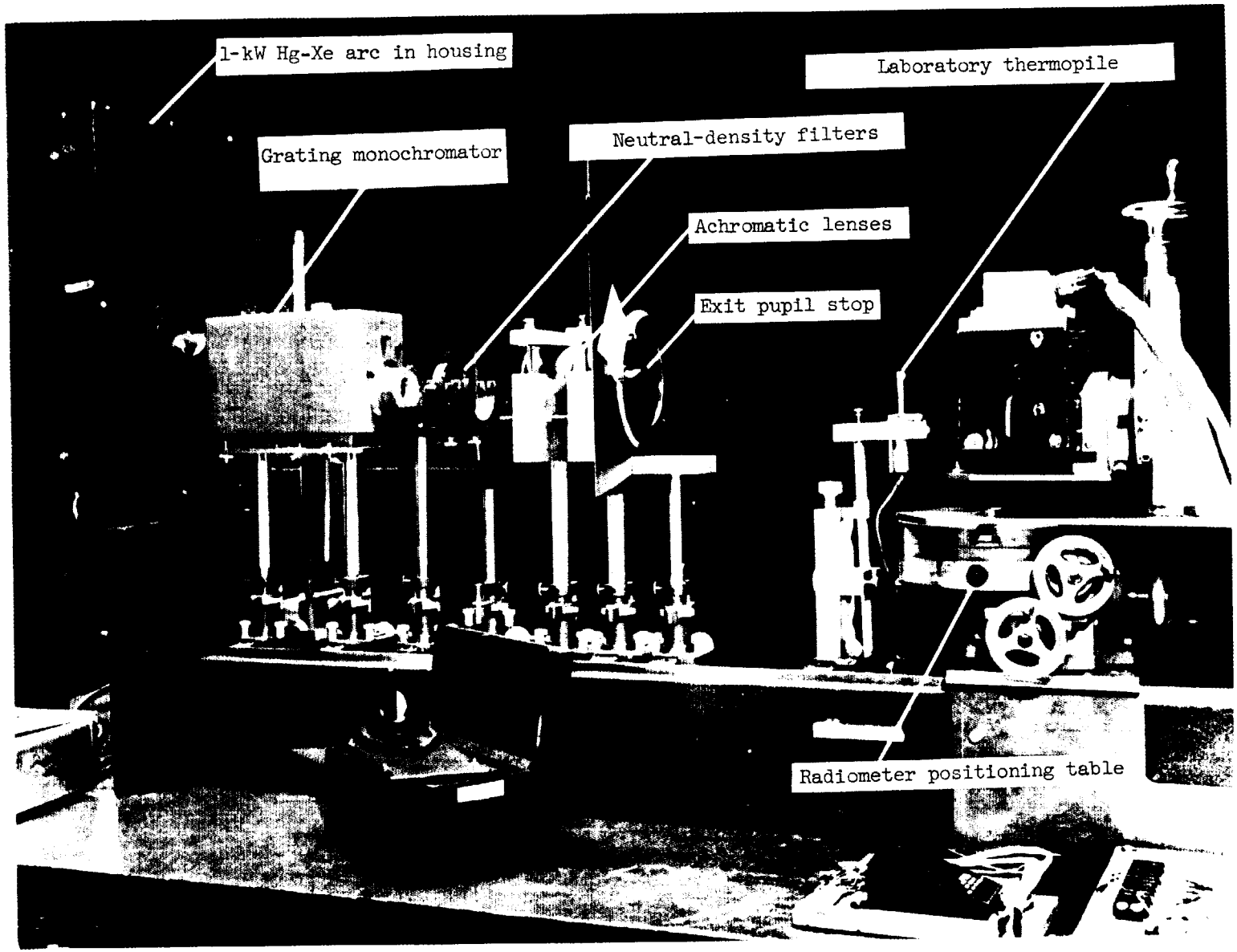

Figure 20.- Monochromatic calibration apparatus for spectral radiometer.

L-66-4454

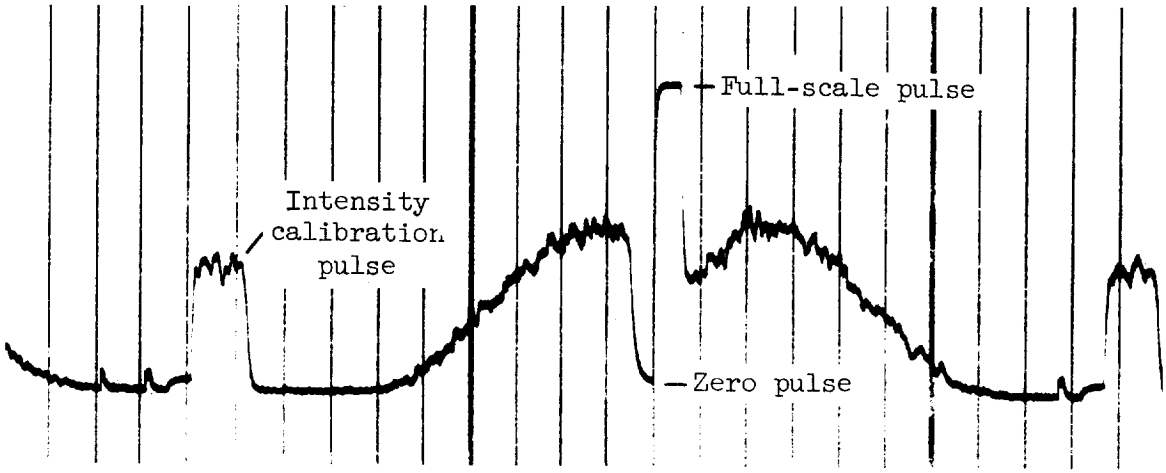

(a) Continuum calibration record at maximum available steradiancy.

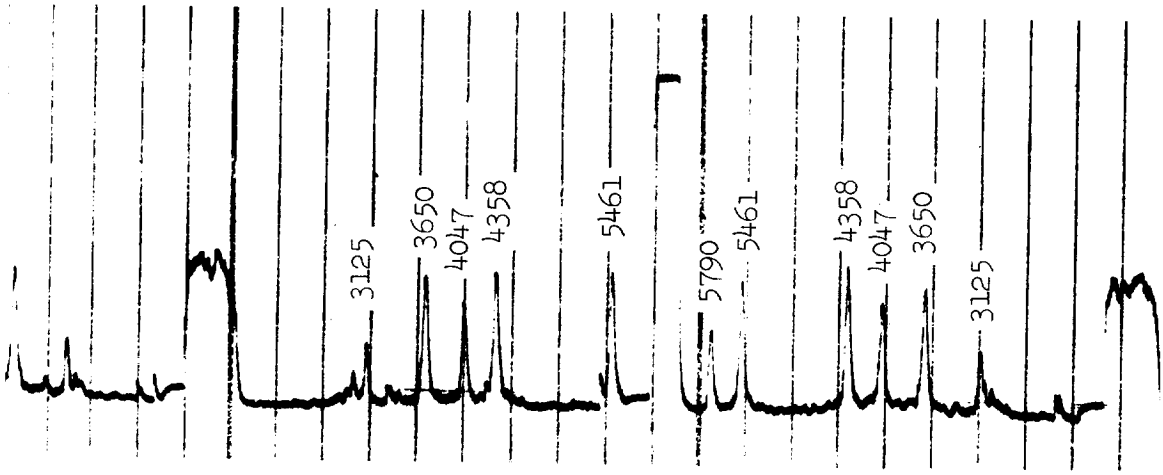

(b) Scan of mercury lamp for wavelength calibration.

Figure 21.- Reproduction of spectral-radiometer calibration records.

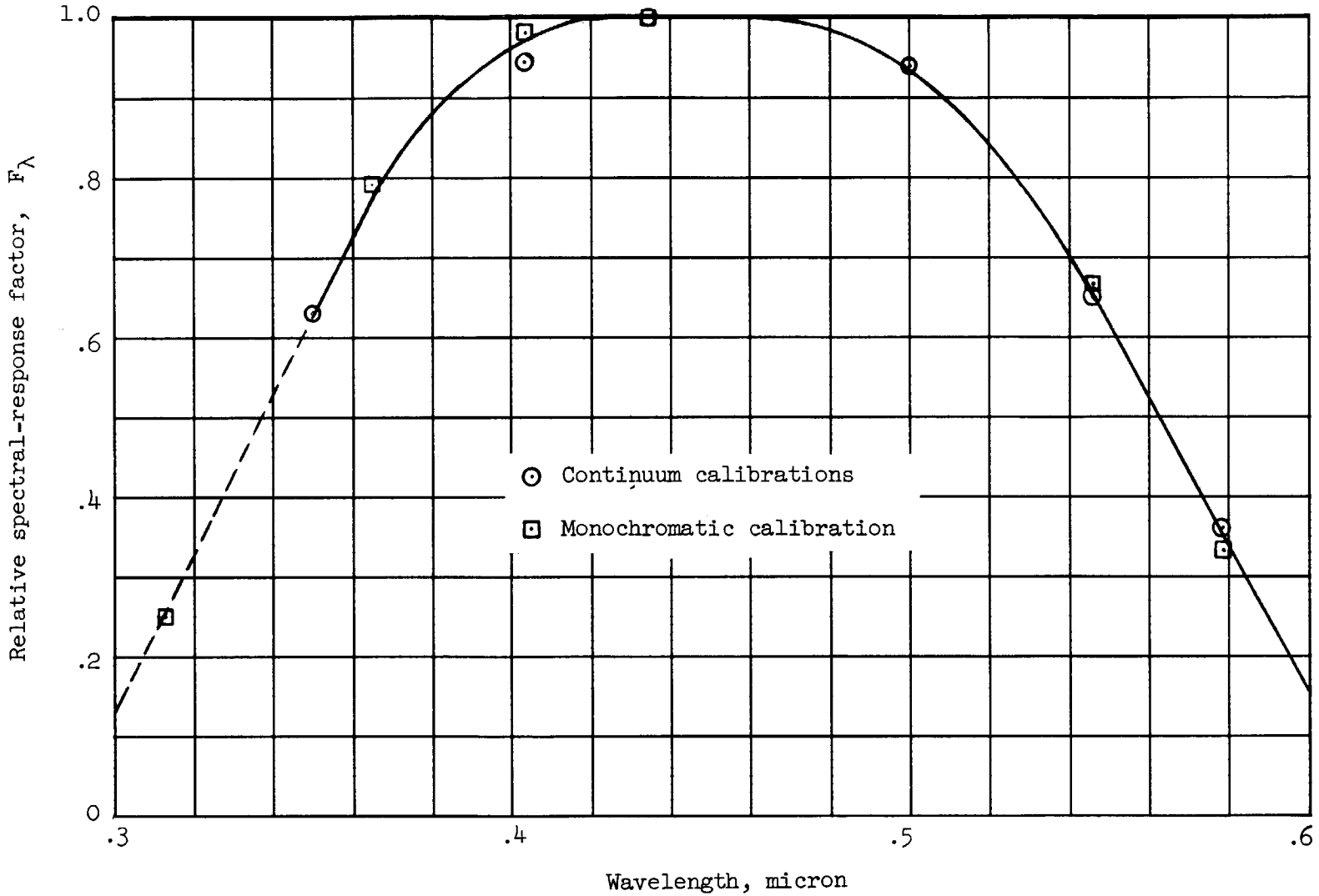

Figure 22.- Relative spectral response of spectral radiometer.

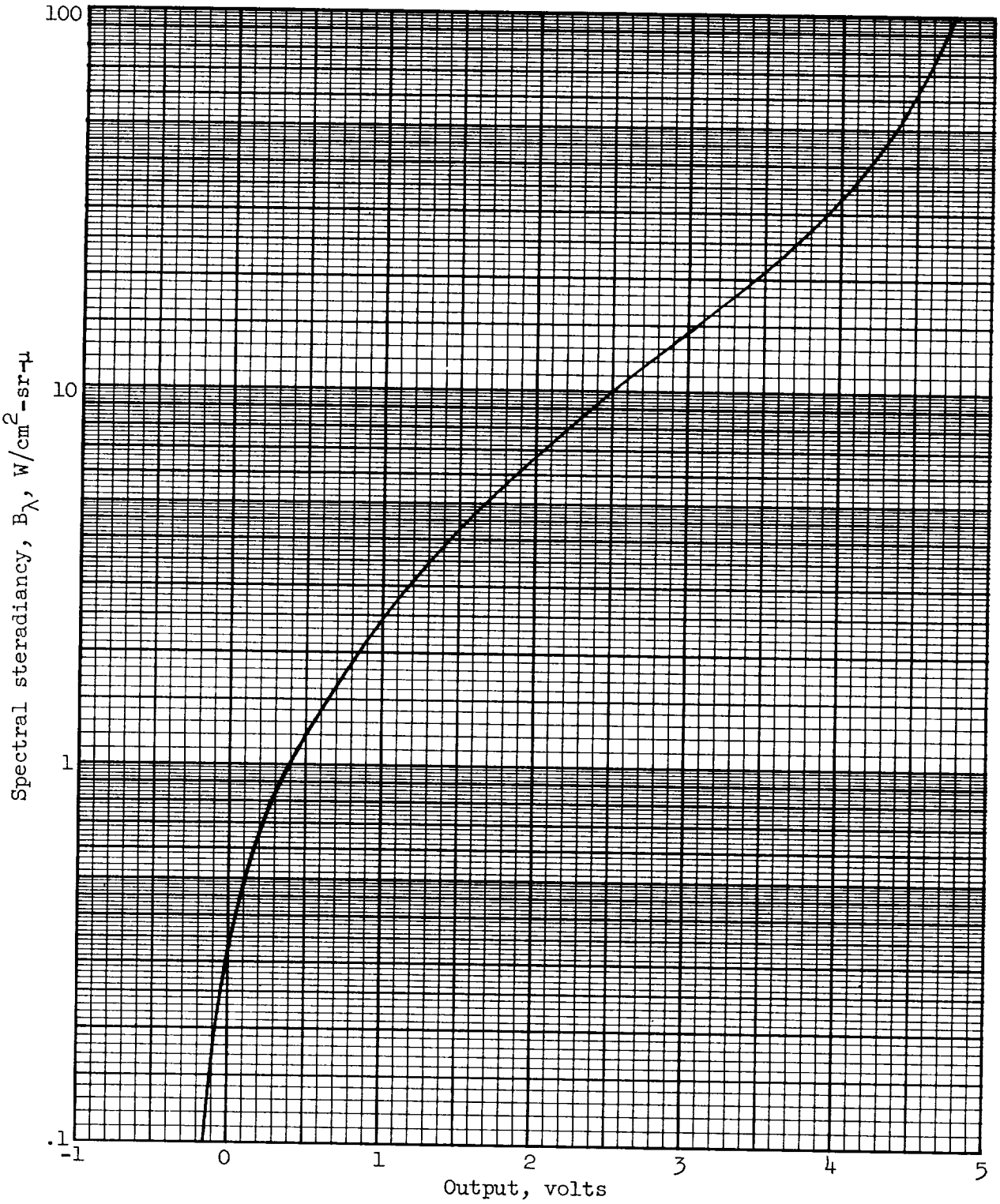

Figure 23.- Spectral-steradiancy calibration of spectral radiometer for wavelength of 0.435 μ.

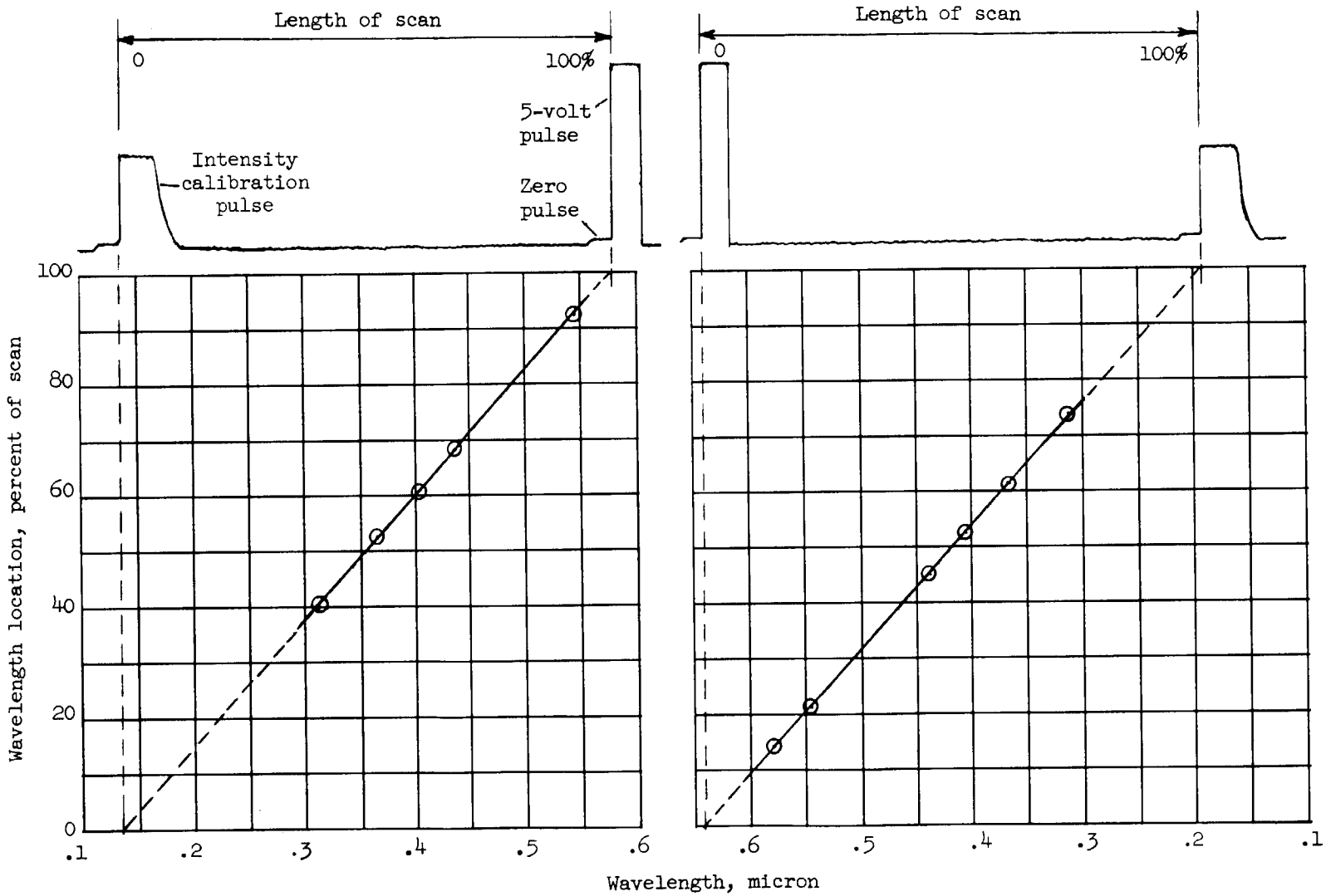

Figure 24.- Spectral-radiometer wavelength calibration.

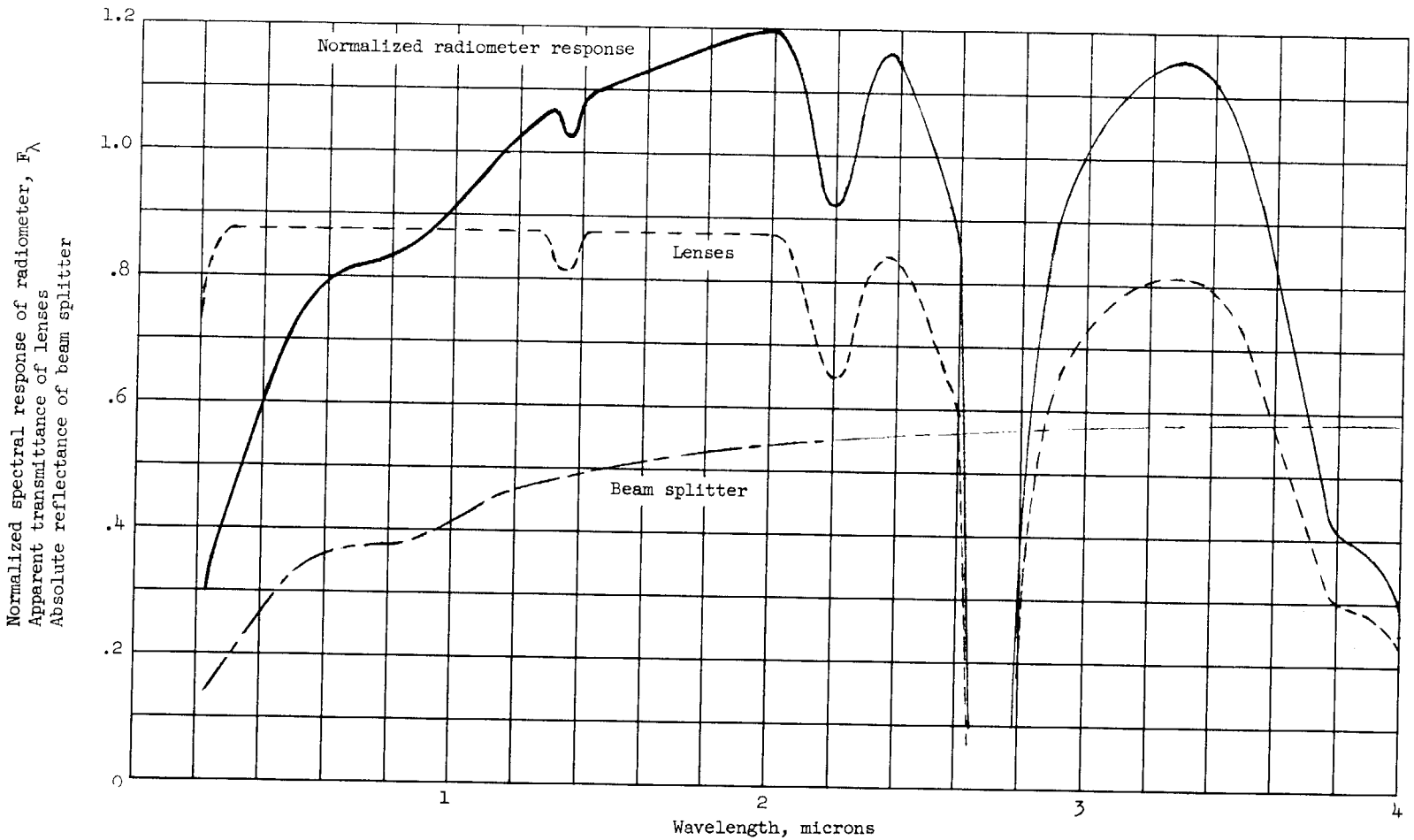

Figure 25.- Normalized spectral response of stagnation total radiometer and characteristics of optical elements.

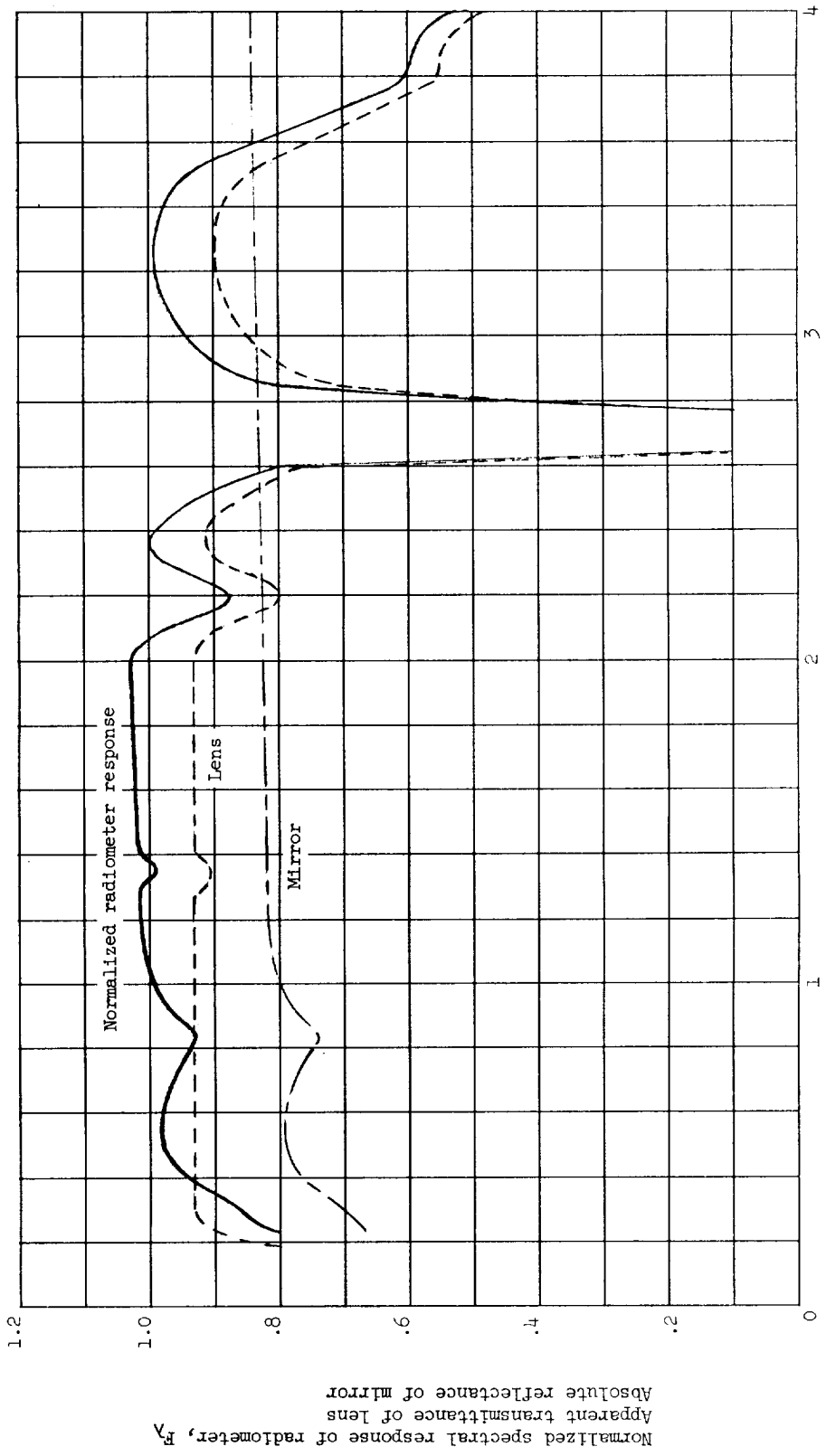

Figure 26.- Normalized spectral response of offset total radiometer and characteristics of optical elements.

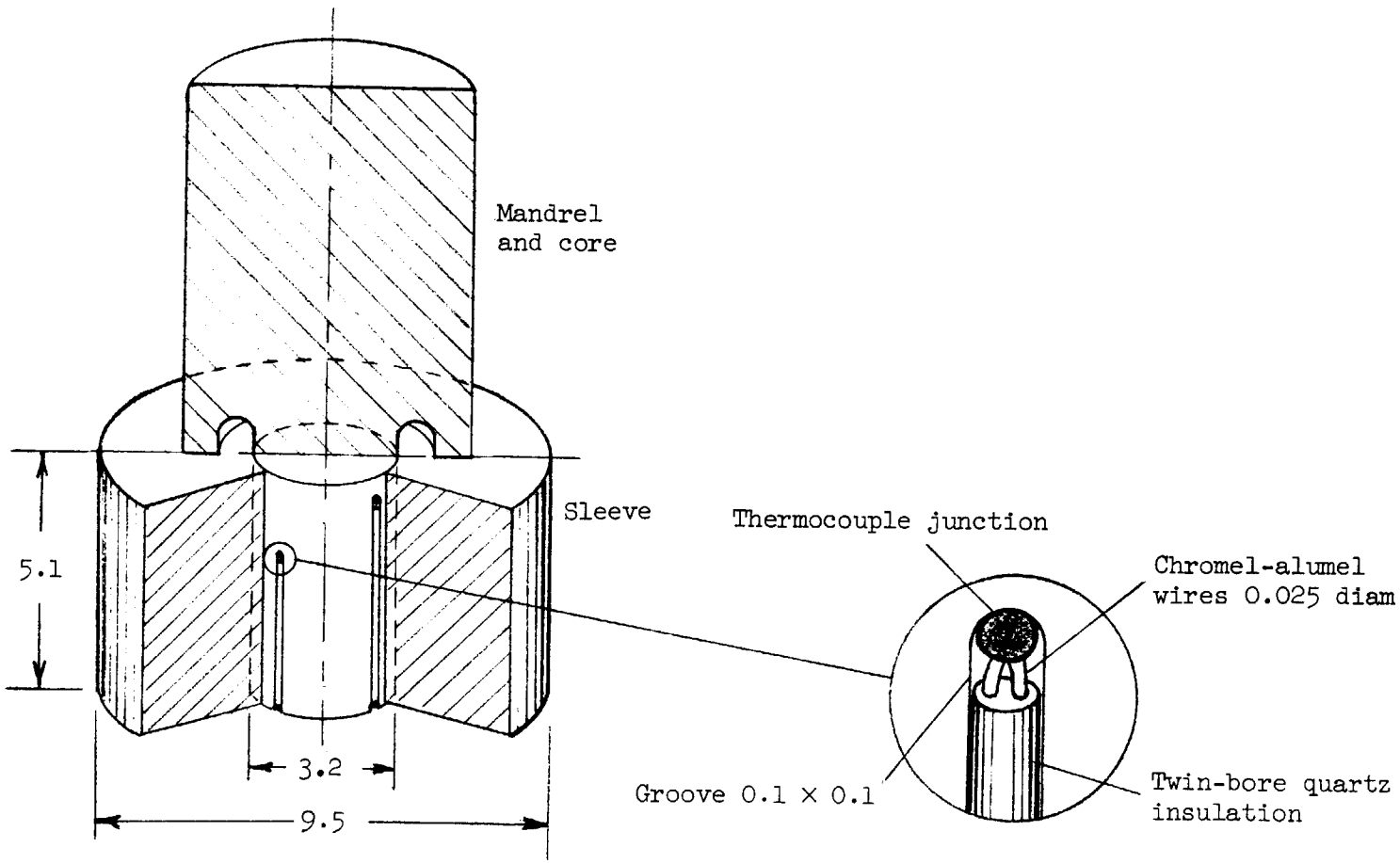

Figure 27.- Details of thermocouple plug for beryllium calorimeters. All dimensions are in mm.

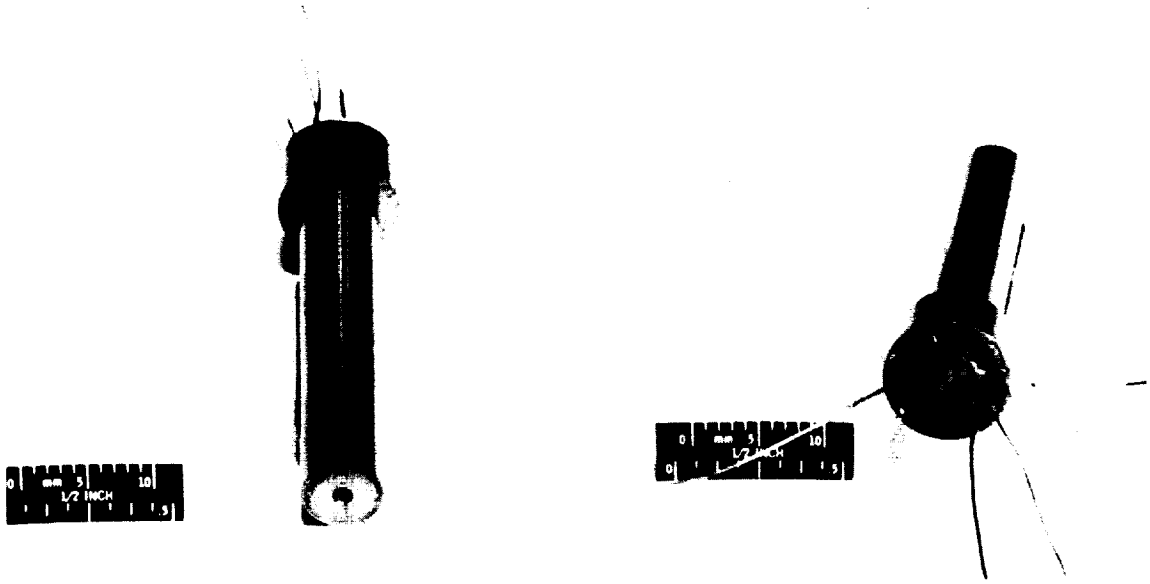

(a) Completed plugs ready for installation.

(b) Photomicrograph of thermocouple junction after removal of sleeve. Magnification about X 300.

Figure 28.- Photographs of thermocouple plugs. L-66-4455

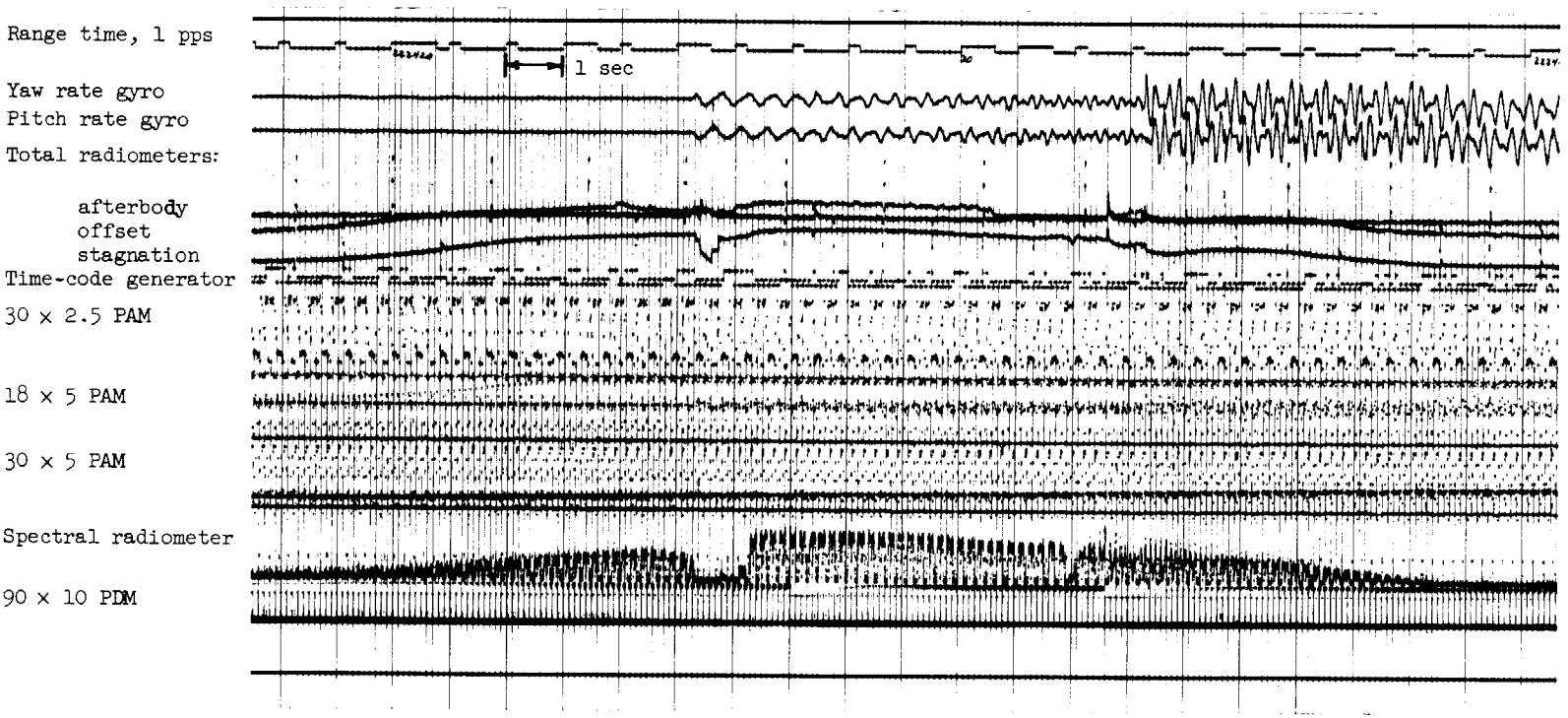

Figure 29.- Reproduction of low-speed oscillograph record of reentry period data.

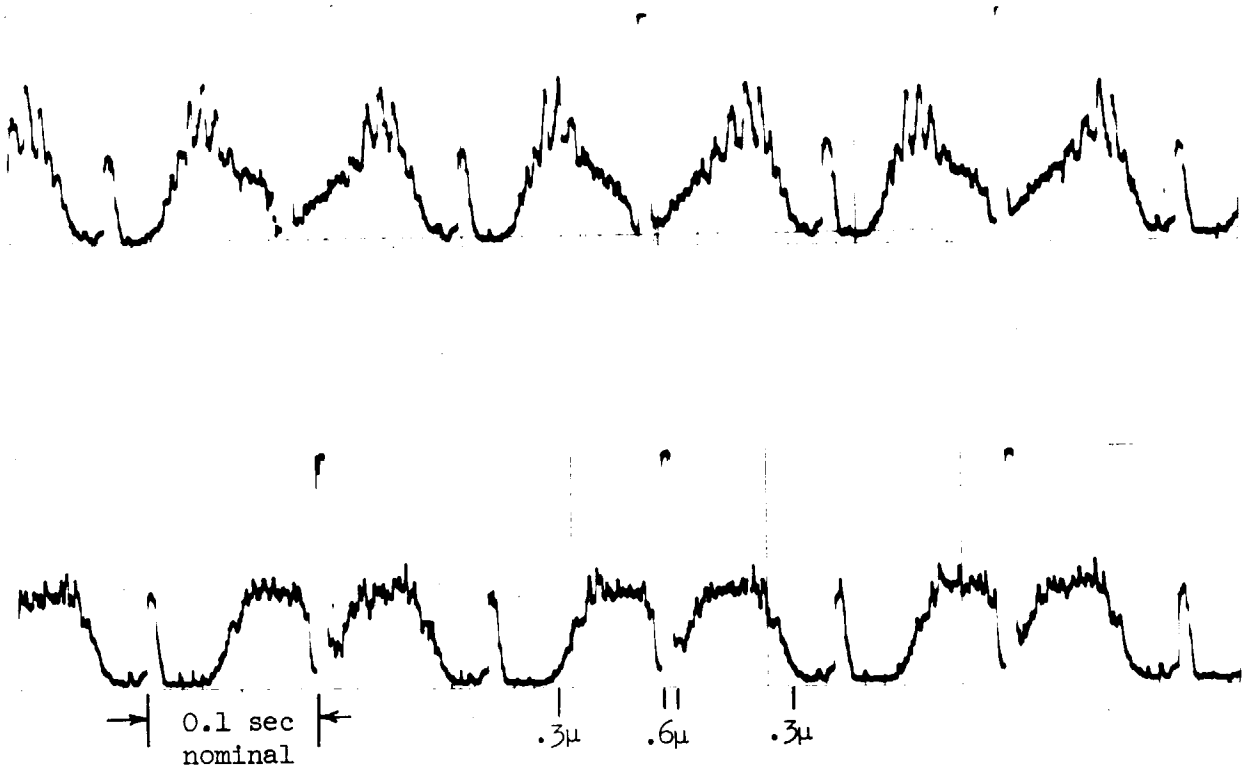

Figure 30.- Reproduction of sections of oscillograph record of spectral-radiometer output during reentry.

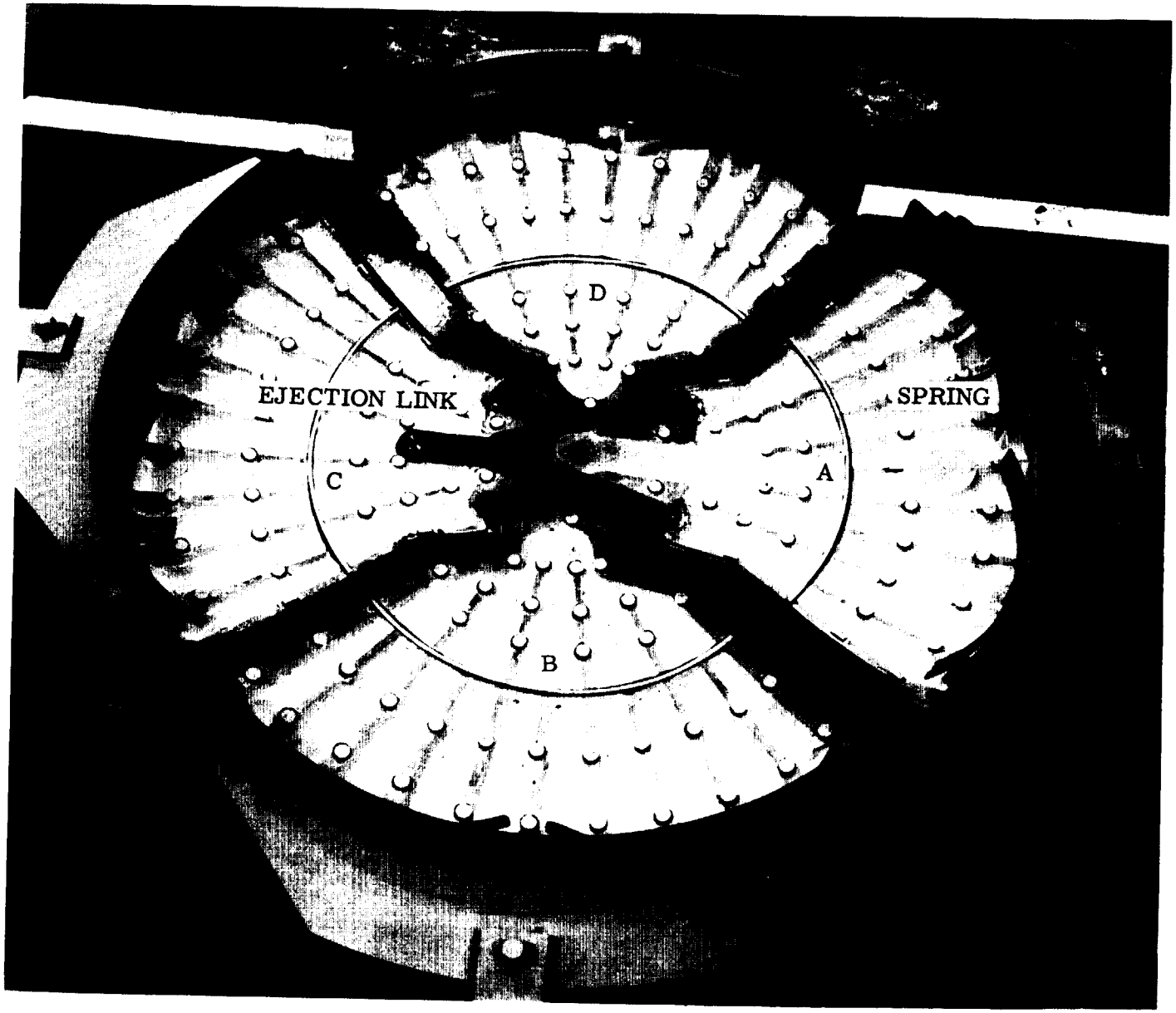

Figure 31.- Phenolic-asbestos heat-shield quadrants in assembly test fixture.

L-66-4456

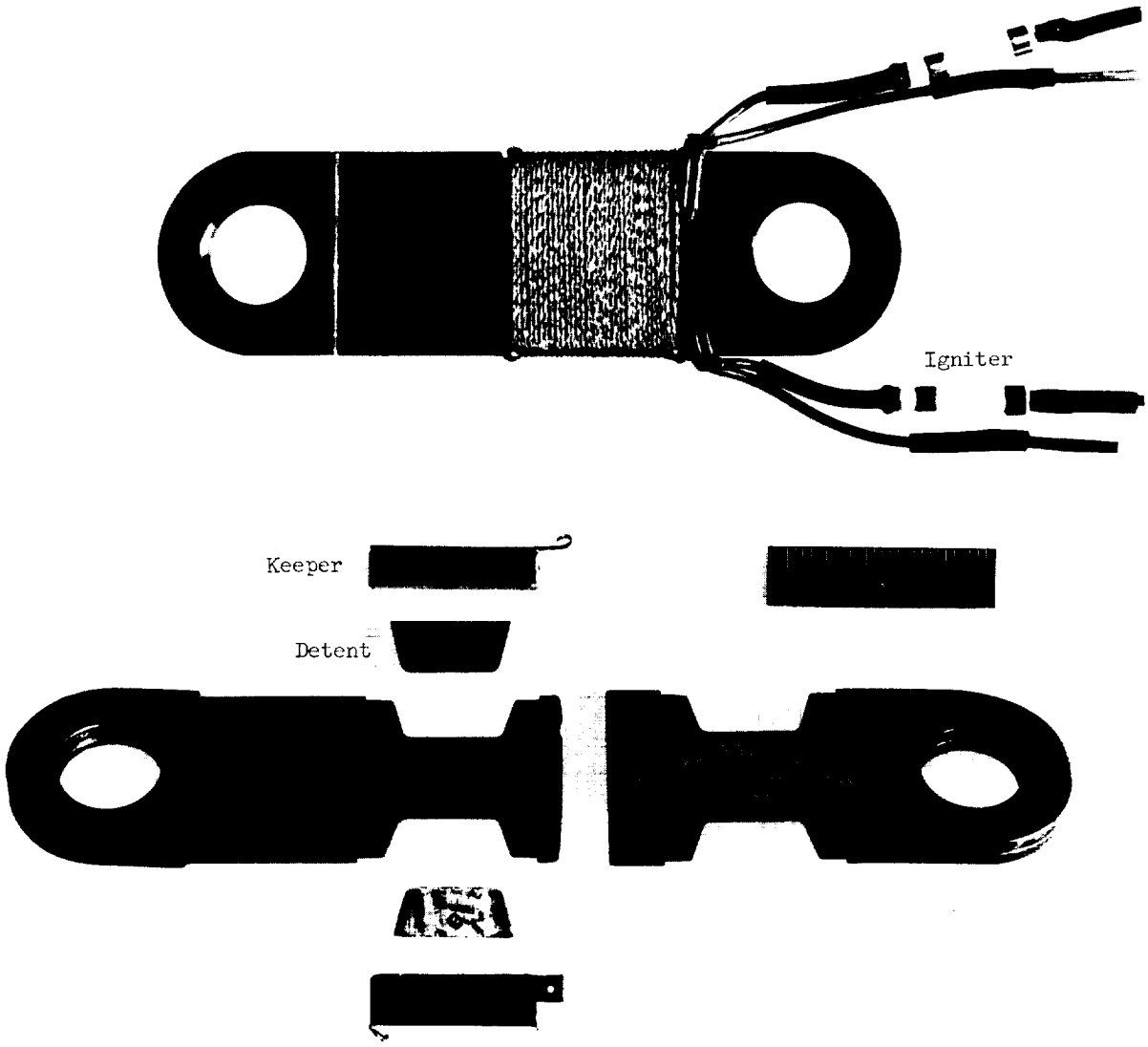

Figure 32.- Photographs of assembled heat-shield ejection link and parts. L-66-4457

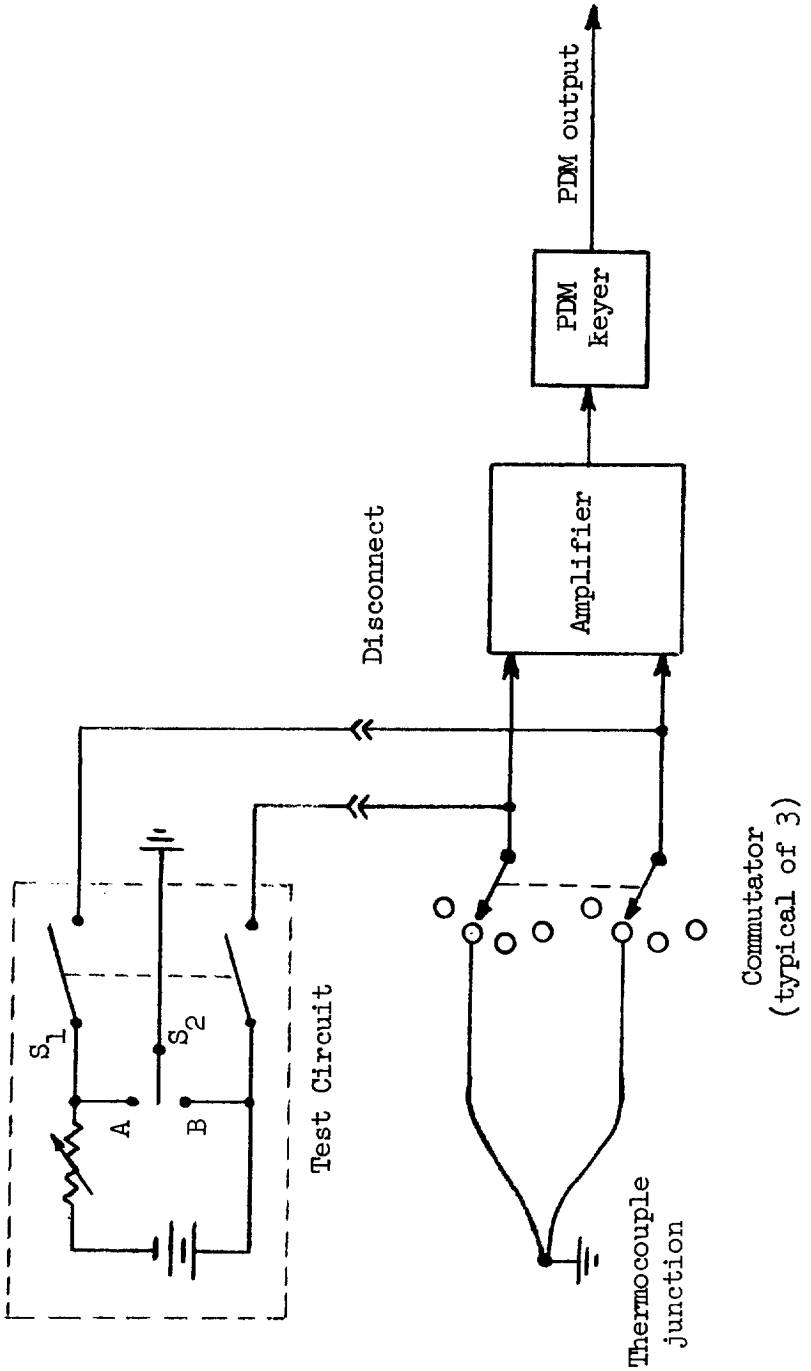

Figure 33.- Test circuit used with PDM system for thermocouple ring-out.

NASA-Langley, 1966 L-4924